Measurement strategies for geoelectrical tomography: Specialized techniques for multichannel instruments

David Belfrage

December 2017

Contents

1 Abstract **3**

2 Introduction to Electrical Resistivity Tomography **4**

3 Problem description, non-theoretical **5**

4 Background **6**
4.1 The sensitivity function 6
4.1.1 The 3D sensitivity function of a homogeneous half-space . 13
4.1.2 The 2D sensitivity function 13
4.1.3 The 1D sensitivity function 15
4.2 Geometrical factor 15
4.3 The tomographic or inversion problem 16
4.4 Number of possible measurements and different kinds of measurements 17
4.5 Previous research 18

5 Theory **18**
5.1 Notation 18
5.2 Problem description, mathematical formulation 19
5.3 Formulation as an optimization problem 19

6 Considered methods **20**
6.1 The integral or sum as a goalfunctions 20
6.2 Spread of center of mass 21
6.3 Correlation 22

7 Multichannel measurements **25**

8 Implementation **34**
8.1 Electrode layout 34
8.1.1 Pre-processing 35
8.2 Calculation of sensitivity 35
8.3 Res2dinv and Res2dmod 36
8.4 Maximum integral, maximum ratio integral 36
8.5 Correlation 37
8.6 Spread mass centers 37
8.7 Multichannel measurements 38
8.8 Correlation multichannel method 41
8.9 Spread mass centers multichannel method 42

9 Results **42**
9.1 Sensitivity patterns 42
9.2 Simulations 47
9.2.1 Results for a 64 electrode array 48
9.2.2 Results for a 30 electrode array 58
9.3 Effectiveness of Multichannel optimization 63
9.4 Field measurements 64

10 Conclusion **68**

11 Outlook and further research **68**

1 Abstract

How to select which measurements to make during a geoelectrical resistivity survey has been an active field of research for decades. Despite this techniques for optimizing the measurement sequences so as to take full advantage of the multichannel capabilities of modern state of the art equipment are scarce. In this thesis special attention is directed towards full usage of the measuring system's multichannel capabilities. The thesis also aims to be an introduction to the field of geoelectrical tomography for the unfamiliar reader, in particular the concept of the sensitivity of a measurement is fully derived. The methods presented in this article are all relying on sampling the sensitivity function and from these samples design a set of measurements. The methods discussed will largely rely on selecting measurements that are as 'different' from eachother as possible — where the difference is measured in either the correlation of the sensitivities or the distance of the sensitivities' mass centers. These new methods are later adapted for multichannel use, after a presentation of how the multichannel system works.

The resulting sets of measurements are tested on a simple model consisting of resistive prisms buried in otherwise homogeneous ground. The simulated measurements and the inversion of these measurements are done with the third party programs res2dmod and res2dinv respectively. From these simulation it is concluded that the methods optimized for multichannel successfully schedules close to the maximum number of measurements per current injection without losing much performance compared to their single channel counterpart. Field measurements with a multichannel-optimized protocol is also presented and compared with a reference protocol.

2 Introduction to Electrical Resistivity Tomography

As this text might have readers with varying backgrounds a brief introduction is given to the general ideas behind Electrical Resistivity Tomography and some terminology. Electrical Resistivity Tomography (ERT) is a method for estimating the resistivity of the subsurface. The end goal is to approximate the resisitivty in order to draw some geological conclusions about the materials in the subsurface by measuring electrical quantities on the surface. To do this some basic tools are required:

1. A current source, preferably one that can give constant current.
2. A voltmeter for measuring potential differences.
3. Electrodes — simple conductive rods that can be hammered into the ground (typically 15-30 centimeters)
4. Wiring to connect two of the electrodes to the current source and two of the electrodes to the voltmeter.

This is what is required for the most basic measurement. A more modern tool called a *terrameter* combines current source and voltmeter into one while also providing many 'quality-of-life' improvements for the personnel responsible for making the field surveys. The most important imporvements concerning this thesis are:

1. The ability to connect many electrodes to the terrameter from which the instrument then selects two electrodes for current injection and two electrodes for potential readings according to a pre-defined protocol.
2. The ability to measure the potential difference between many pair of electrodes for every current injection (this is what is called *multichannel capabilities*).

With only the most basic tool we would have to change which pair of electrodes to use for current injection and which pair of electrodes to use for potential reading manually, the terrameter automates this process entirely.

Geoelectrical resistivity measurements, what is it?

A geoelectrical measurement uses four electrodes — two for injecting current and two for measuring the potential difference. By knowing the current, the measured potential difference, the electrode positions and assuming that the ground has a homogeneous resistivity distribution an estimation of the resistivity in the ground can be made. The resisitivity value calculated in this way is called *apparent resistivity* which represents the resisitivity the ground would have if the hypothesis of homogeneous ground was correct [1, 6]. In most practical

cases the ground is not homogeneous which makes it necessary to make more than one measurement in order to get a good image of the subsurface resistivity distribution.

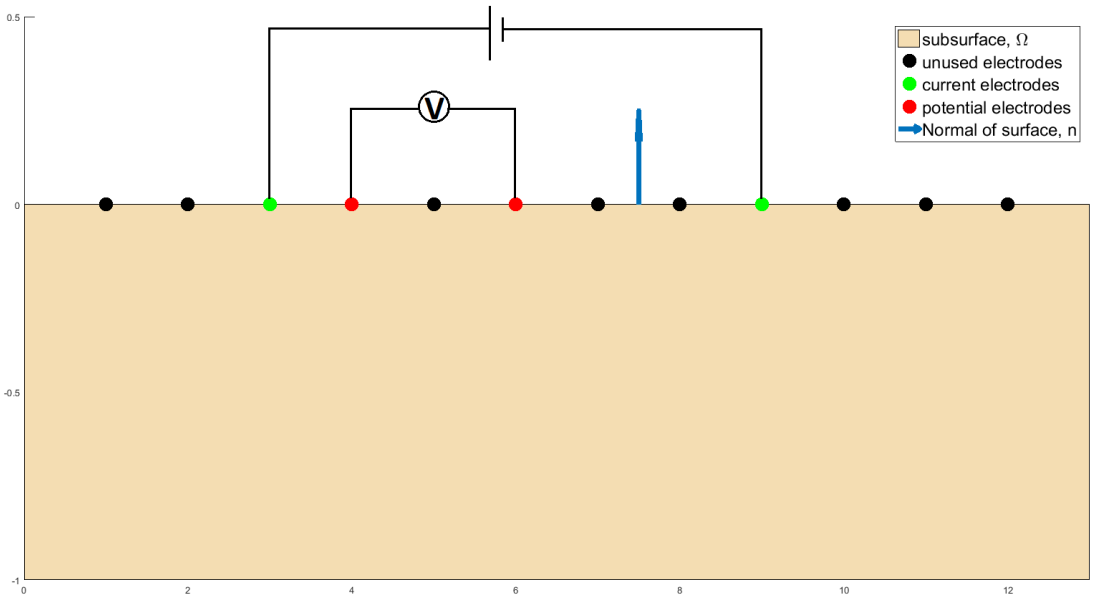

Figure 1: This is a simplified view of the problem at hand. The light brown subsurface has an unknown resistivity distribution. In order to estimate it we have planted electrodes into the subsurface. We use a current source connected to two electrodes (green) and measure the resulting potential difference with a voltmeter between two electrodes (red). The rest of the electrodes are unused for this measurement (black). The notation Ω and $\mathbf{n}$ will be used later, for more mathematical concepts.

In Figure 1 we see a simple setup — the twelve electrodes are connected to a terrameter, two of these are used for current injections while two other are used for potential readings (the rest of the electrodes are unused for this particular measurement).

3 Problem description, non-theoretical

When doing state of the art electric resistivity surveys of the subsurface a high number of electrodes are often in use. Each measurement uses four electrodes — two for injecting current and two for measuring the potential difference. The

total number of possible measurements exhibits fourth order growth with the number of electrodes. For an electrode layout of 64 electrodes this would be over a million possible measurements. Due to time constraints and the cost of the deploying personnel in the field, all the possible measurements are very seldomly taken. Instead a much smaller subset of all these measurements, consisting of at most a couple of thousand measurements, is usually what is measured in the field. For a long time the set of measurements that were used was selected from a set of standard measurements — measurements that for some reason were easily deployed. The advancements in field equipment and computer technology has however opened up new possibilities. With computers it is easier to evaluate *all* possible measurements before going out in the field. The field equipment can take more than one measurement at a time leading either to better survey qualities, due to more data points, or to faster data acquisition. Specialized techniques are however needed to design sets of measurements that uses the multichannel capabilities of the instruments to their full, or close to their full, potential.

The goal of this thesis is hence twofold: how do you select amongst this vast set of possible measurements and how should we select measurements so that the multichannel capabilities of the measuring equipment is used to a large extent?

4 Background

4.1 The sensitivity function

If the subsurface is homogeneous any measurement, assuming it to be noise free, would be able to correctly estimate the resistivity of the ground. In the real world the subsurface is never homogeneous (nor are the measurements noise free) and different measurements will be sensitive to changes in the subsurface resistivity distribution in different ways. This should be at least a little bit intuitive: a potential measurement should be more heavily impacted by a change in the resistivity near the electrodes than one very far away. This section is meant to give a little mathematical rigor to this intuition. If one is very familiar with the concept of sensitivity for geoelectrical resisitivty measurements this section can be skimmed or skipped. For the very interested reader similar derivations as the one presented below exist for more general cases [5, 7].

The fundamental partial differential equation

We will begin this journey from a very general case, the ground or subsurface is thought of as a domain $\Omega \subset \mathbf{R}^3$ with a boundary $\partial\Omega$, the current is injected by a function I acting along the boundary $\partial\Omega$ and no other current sources exist in Ω. In the following equations ρ denotes the resistivity distribution over Ω, $\mathbf{J}$ denotes the current density, ϕ denotes the electrical potential and $\mathbf{n}$ denotes the normal of the boundary. Armed with this notation the following fundamental

formulas of electrostatics holds [2]:

$$\begin{cases} \nabla \cdot \mathbf{J}(\mathbf{x}) = 0 & \text{for } \mathbf{x} \in \Omega \\ \mathbf{J} \cdot \mathbf{n} = I(\mathbf{x}) & \text{for } \mathbf{x} \in \partial\Omega \end{cases}$$

which is the continuity equation for electric charge and Ohm's Law:

$$\mathbf{J} = -\frac{1}{\rho(\mathbf{x})} \nabla \phi(\mathbf{x}).$$

By inserting the last equation, relating the current density with the potential, into the boundary conditions and divergence criteria for the current density we get:

$$\begin{cases} -\nabla \cdot \left(\frac{1}{\rho(\mathbf{x})} \nabla \phi(\mathbf{x}) \right) = 0 & \text{for } \mathbf{x} \in \Omega \\ -\frac{1}{\rho(\mathbf{x})} \nabla \phi(\mathbf{x}) \cdot \mathbf{n} = I(\mathbf{x}) & \text{for } \mathbf{x} \in \partial\Omega \end{cases} \tag{1}$$

This is the partial differential equation (PDE) that the electrical potential with inhomogeneous Neumann boundary conditions have to follow. The PDE in (1) will be refered to as the *Fundamental PDE*. Note that the solution to the fundamental PDE is only determined up to a constant, in practice this does not matter as only differences of the potential is examined. In practice the current injection I should also integrate to zero if Ω is bounded i.e.

$$\int_{\partial\Omega} I(x) \, \mathrm{dS} = 0 \tag{2}$$

since the current injected in to Ω cannot be destroyed due to the assumptions of no sources or sinks in Ω.

Let's drop the general case for a brief moment, and instead study the special case where

$$\begin{aligned} \Omega &= \left\{ \mathbf{x} = (x, y, z) \in \mathbb{R}^3 | z < 0 \right\} \\ \partial\Omega &= \left\{ \mathbf{x} \in \mathbb{R}^3 | z = 0 \right\} \\ \rho(\mathbf{x}) &= \rho_0 \\ I(\mathbf{x}) &= \delta(\mathbf{x} - \mathbf{x}_c), \end{aligned}$$

i.e. the when the resistivity is homogeneous and a point current source is injecting 1 Ampere at $\mathbf{x}_c \in \partial\Omega$. The fundamental PDE becomes

$$\begin{cases} -\nabla^2 \phi(\mathbf{x}) = 0 & \text{for } \mathbf{x} \in \Omega \\ -\frac{1}{\rho_0} \nabla \phi(\mathbf{x}) \cdot \mathbf{n} = \delta(\mathbf{x} - \mathbf{x}_c) & \text{for } \mathbf{x} \in \partial\Omega \end{cases} \tag{3}$$

which has a unique solution if we for example assume that $|\phi|$ tend to zero as we move infinitely far away from the current source. The solution is

$$\phi = \frac{\rho}{2\pi|\mathbf{x} - \mathbf{x}_c|}. \tag{4}$$

This I does not however fulfill the condition that it should integrate to zero along the surface — in order to remedy this we can add a negative source as well:

$$\begin{cases} -\nabla^2\phi(\mathbf{x}) = 0 & \text{for } \mathbf{x} \in \Omega \\ -\dfrac{1}{\rho_0}\nabla\phi(\mathbf{x}) \cdot \mathbf{n} = \delta(\mathbf{x} - \mathbf{x}_{c1}) - \delta(\mathbf{x} - \mathbf{x}_{c2}) & \text{for } \mathbf{x} \in \partial\Omega \end{cases} \tag{5}$$

but the solution is given by simply adding solutions as in (4) with opposite signs i.e.

$$\phi = \frac{\rho}{2\pi|\mathbf{x} - \mathbf{x}_{c1}|} - \frac{\rho}{2\pi|\mathbf{x} - \mathbf{x}_{c2}|} = \frac{\rho}{2\pi}\left(\frac{1}{|\mathbf{x} - \mathbf{x}_{c1}|} - \frac{1}{|\mathbf{x} - \mathbf{x}_{c2}|}\right). \tag{6}$$

Potential measurements and perturbations of resistivity

So far we have only introduced concepts relating to how the current injection into Ω is made, in this section a *potential measurement* will be introduced. The potential measurement can be imagined as a linear functional over the boundary of Ω:

$$\begin{cases} F(\phi) = \displaystyle\int_{\partial\Omega} g(\mathbf{x})\phi(\mathbf{x})\,\mathrm{dS} \\ F(1) = \displaystyle\int_{\partial\Omega} g(\mathbf{x})\,\mathrm{dS} = 0 \end{cases} \tag{7}$$

the extra assumption of $F(1) = 0$ makes sure that an added constant to the potential ϕ does not influence the measurement. This is important as the potential is only determined up to a constant! For now we stick with very general notation in (7), but normally $g(\mathbf{x})$ is a positive and negative Dirac delta function located somewhere on $\partial\Omega$ such that the potential measurement is the difference in potential between two points i.e.

$$F(\phi) = \int_{\partial\Omega} \left(\delta(\mathbf{x} - \mathbf{x}_1) - \delta(\mathbf{x} - \mathbf{x}_2)\right)\phi(\mathbf{x})\,\mathrm{dS} = \phi(\mathbf{x}_1) - \phi(\mathbf{x}_2). \tag{8}$$

In order to introduce the sensitivity of a measurement we will make a perturbation of the resistivity and see what effect this will have on the potential measurement. Let's introduce a perturbation to the resistivity as follows:

$$\rho_t = \rho + t\tilde{\rho},$$

where $\tilde{\rho}$ is a function defined on Ω. We can think of $\tilde{\rho}$ as a basis for the perturbation, it is the shape with which we wish to make a small change in the resistivity. We could add further demands on $\tilde{\rho}$, such as it integrating to 1 in order to get an interpretation of t as a scaling factor. The support of $\tilde{\rho}$

should be on the interior of Ω as we do not want to handle variations close to the boundary (in practise close to the electrodes on the boundary). We can of course solve the fundamental PDE for this new resistivity distribution as well:

$$\begin{cases} -\nabla \cdot \left(\dfrac{1}{\rho_t(\mathbf{x})} \nabla \phi_t(\mathbf{x}) \right) = 0 & \text{for } \mathbf{x} \in \Omega \\ -\dfrac{1}{\rho_t(\mathbf{x})} \nabla \phi_t(\mathbf{x}) \cdot \mathbf{n} = I(\mathbf{x}) & \text{for } \mathbf{x} \in \partial\Omega \end{cases} \tag{9}$$

where ϕ_t denotes the new electrical potential arising from the perturbation of the resistivity. We want to study how this potential changes with t — in particular we want to know

$$\left. \frac{\partial F(\phi_t)}{\partial t} \right|_{t=0} = F\left(\left. \frac{\partial \phi_t}{\partial t} \right|_{t=0} \right) = F(\tilde{\phi})$$

which we will define as the *response* of the potential measurement to a small change in resistivity. Obviously this will depend on the the form of $\tilde{\rho}$, the 'basis' of perturbation, but for now the form of $\tilde{\rho}$ is left unspecified. In order to find $\tilde{\phi} = \left. \frac{\partial \phi_t}{\partial t} \right|_{t=0}$ we take the derivative with respect to t on (9):

$$\begin{cases} \dfrac{\partial}{\partial t} \left(-\nabla \cdot \left(\dfrac{1}{\rho_t(\mathbf{x})} \nabla \phi_t(\mathbf{x}) \right) \right) = 0 & \text{for } \mathbf{x} \in \Omega \\ \dfrac{\partial}{\partial t} \left(-\nabla \phi_t(\mathbf{x}) \cdot \mathbf{n} \right) = \dfrac{\partial}{\partial t} \left(\rho_t(\mathbf{x}) I(\mathbf{x}) \right) & \text{for } \mathbf{x} \in \partial\Omega \end{cases} \tag{10}$$

we change the order of differentiation so that we differentiate with respect to t first and then take the spatial derivatives :

$$\begin{cases} -\nabla \cdot \left(\dfrac{1}{\rho_t(\mathbf{x})^2} \left(\rho_t(\mathbf{x}) \nabla \dfrac{\partial \phi_t(\mathbf{x})}{\partial t} - \tilde{\rho}(\mathbf{x}) \nabla \phi_t(\mathbf{x}) \right) \right) = 0 & \text{for } \mathbf{x} \in \Omega \\ -\nabla \dfrac{\partial \phi_t(\mathbf{x})}{\partial t} \cdot \mathbf{n} = \tilde{\rho}(\mathbf{x}) I(\mathbf{x}) & \text{for } \mathbf{x} \in \partial\Omega \end{cases} \tag{11}$$

Insertion of $t = 0$ yields:

$$\begin{cases} -\nabla \cdot \left(\dfrac{1}{\rho(\mathbf{x})^2} \left(\rho(\mathbf{x}) \nabla \tilde{\phi}(\mathbf{x}) - \tilde{\rho}(\mathbf{x}) \nabla \phi(\mathbf{x}) \right) \right) = 0 & \text{for } \mathbf{x} \in \Omega \\ -\nabla \tilde{\phi}(\mathbf{x}) \cdot \mathbf{n} = \tilde{\rho}(\mathbf{x}) I(\mathbf{x}) & \text{for } \mathbf{x} \in \partial\Omega \end{cases} \tag{12}$$

where, as before, $\tilde{\phi} = \left. \frac{\partial \phi_t}{\partial t} \right|_{t=0}$, the quantity $\tilde{\phi}$ could be interpreted as a the small change in the potential resulting from a small perturbation in the resistivity.

The response function

The PDE presented in (12) governs how the potential changes due to the small perturbation in resistivty. We could aim to solve this directly, but that looks like

a daunting task. Instead we will use a neat trick, related to the adjoint equation of (12) to get a familiar PDE. We begin by multiplying the governing equation with a test function w and integrating, this will give us the weak formulation:

$$\begin{aligned}
0 &= \int_\Omega -\nabla \cdot \left(\frac{1}{\rho(\mathbf{x})^2} \left(\rho(\mathbf{x}) \nabla \tilde{\phi}(\mathbf{x}) - \tilde{\rho}(\mathbf{x}) \nabla \phi(\mathbf{x}) \right) \right) w \, \mathrm{dV} \\
&= - \int_{\partial\Omega} \frac{1}{\rho(\mathbf{x})^2} \left(\rho(\mathbf{x}) \nabla \tilde{\phi}(\mathbf{x}) - \tilde{\rho}(\mathbf{x}) \nabla \phi(\mathbf{x}) \right) w \cdot \mathbf{n} \, \mathrm{dS} \\
&\quad + \int_\Omega \frac{1}{\rho(\mathbf{x})^2} \left(\rho(\mathbf{x}) \nabla \tilde{\phi}(\mathbf{x}) - \tilde{\rho}(\mathbf{x}) \nabla \phi(\mathbf{x}) \right) \cdot \nabla w \, \mathrm{dV}.
\end{aligned}$$

By insertion of the boundary conditions on ϕ and $\tilde{\phi}$ the surface integral is zero, and we are left with:

$$\begin{aligned}
0 &= \int_\Omega \frac{1}{\rho(\mathbf{x})^2} \left(\rho(\mathbf{x}) \nabla \tilde{\phi}(\mathbf{x}) - \tilde{\rho}(\mathbf{x}) \nabla \phi(\mathbf{x}) \right) \cdot \nabla w \, \mathrm{dV} \\
&= \int_\Omega \frac{1}{\rho(\mathbf{x})} \nabla \tilde{\phi}(\mathbf{x}) \cdot \nabla w \, \mathrm{dV} - \int_\Omega \frac{\tilde{\rho}(\mathbf{x})}{\rho(\mathbf{x})^2} \nabla \phi(\mathbf{x}) \cdot \nabla w \, \mathrm{dV}.
\end{aligned} \tag{13}$$

We can integrate the first term by parts:

$$\int_\Omega \frac{1}{\rho(\mathbf{x})} \nabla \tilde{\phi}(\mathbf{x}) \cdot \nabla w \, \mathrm{dV} = \int_{\partial\Omega} \tilde{\phi}(\mathbf{x}) \frac{\nabla w}{\rho(\mathbf{x})} \cdot \mathbf{n} \, \mathrm{dS} - \int_\Omega \tilde{\phi}(\mathbf{x}) \nabla \cdot \left(\frac{\nabla w}{\rho(\mathbf{x})} \right) \mathrm{dV}$$

and by inserting this into (13) we get:

$$\int_{\partial\Omega} \tilde{\phi}(\mathbf{x}) \frac{\nabla w}{\rho(\mathbf{x})} \cdot \mathbf{n} \, \mathrm{dS} - \int_\Omega \tilde{\phi}(\mathbf{x}) \nabla \cdot \left(\frac{\nabla w}{\rho(\mathbf{x})} \right) \mathrm{dV} - \int_\Omega \frac{\tilde{\rho}(\mathbf{x})}{\rho(\mathbf{x})^2} \nabla \phi(\mathbf{x}) \cdot \nabla w \, \mathrm{dV} = 0. \tag{14}$$

The idea is to move the differentiations away from $\tilde{\phi}$ and onto w, later we will find a special w that will give us the value we are looking for. Remember that we want the value of some linear functional of $\tilde{\phi}$ defined as

$$F(\tilde{\phi}) = F(\tilde{\phi}(\mathbf{x})) = \int_{\partial\Omega} g(\mathbf{x}) \tilde{\phi}(\mathbf{x}) \, \mathrm{dS}.$$

We add and subtract this value from (14) and get:

$$\begin{aligned}
0 &= \int_{\partial\Omega} \tilde{\phi}(\mathbf{x}) \frac{\nabla w}{\rho(\mathbf{x})} \cdot \mathbf{n} \, \mathrm{dS} - \int_\Omega \tilde{\phi}(\mathbf{x}) \nabla \cdot \left(\frac{\nabla w}{\rho(\mathbf{x})} \right) \mathrm{dV} \\
&\quad - \int_\Omega \frac{\tilde{\rho}(\mathbf{x})}{\rho(\mathbf{x})^2} \nabla \phi(\mathbf{x}) \cdot \nabla w \, \mathrm{dV} + \int_{\partial\Omega} g(\mathbf{x}) \tilde{\phi}(\mathbf{x}) \, \mathrm{dS} - \int_{\partial\Omega} g(\mathbf{x}) \tilde{\phi}(\mathbf{x}) \, \mathrm{dS}.
\end{aligned}$$

Rearranging a bit we get:

$$
\begin{aligned}
0 = &\int_{\partial\Omega} \tilde{\phi}(\mathbf{x}) \left(\frac{\nabla w}{\rho(\mathbf{x})} \cdot \mathbf{n} + g(\mathbf{x}) \right) \mathrm{dS} \\
&- \int_{\Omega} \tilde{\phi}(\mathbf{x}) \nabla \cdot \left(\frac{\nabla w}{\rho(\mathbf{x})} \right) \mathrm{dV} \\
&- \int_{\Omega} \frac{\tilde{\rho}(\mathbf{x})}{\rho(\mathbf{x})^2} \nabla \phi(\mathbf{x}) \cdot \nabla w \, \mathrm{dV} \\
&+ \int_{\partial\Omega} g(\mathbf{x}) \tilde{\phi}(\mathbf{x}) \, \mathrm{dS}.
\end{aligned} \tag{15}
$$

Now a clever trick will be used — if we can find a w such that the first two terms are zero for all $\tilde{\phi}$ we see that

$$
F(\tilde{\phi}) = \int_{\partial\Omega} g(\mathbf{x}) \tilde{\phi}(\mathbf{x}) \, \mathrm{dS} = \int_{\Omega} \frac{\tilde{\rho}(\mathbf{x})}{\rho(\mathbf{x})^2} \nabla \phi(\mathbf{x}) \cdot \nabla w \, \mathrm{dV} \tag{16}
$$

i.e the value of $F(\tilde{\phi})$ is given by the solution to the fundamental PDE ϕ and a w such that the two first terms in (15) is zero. The question is now how to find such a w, but this is easily seen to be a w fulfilling the following PDE:

$$
\begin{cases}
-\nabla \cdot \left(\dfrac{\nabla w}{\rho(\mathbf{x})} \right) = 0 & \text{for } \mathbf{x} \in \Omega \\
\dfrac{-\nabla w}{\rho(\mathbf{x})} \cdot \mathbf{n} = g(\mathbf{x}) & \text{for } \mathbf{x} \in \partial\Omega
\end{cases} \tag{17}
$$

but this is the PDE of a electrical potential on the same form as the fundamental PDE! So we have found the response of a measurement as an integral over two solutions of the fundamental PDE with different boundary conditions!

Summary of the results

The derivation so far has been very general and the results can be summerized as: we have shown that for a general domain Ω with a current injection $I(\mathbf{x})$ on the boundary, a variable resistivity $\rho(\mathbf{x})$ and potential measurement defined as a functional:

$$
F(\phi) = \int_{\Omega} g(\mathbf{x}) \phi(\mathbf{x}) \, \mathrm{dV}. \tag{18}
$$

then the response of the functional F to a small perturbation in the resistivity is given by:

$$
F(\tilde{\phi}) = \int_{\Omega} \frac{\tilde{\rho}(\mathbf{x})}{\rho(\mathbf{x})^2} \nabla \phi(\mathbf{x}) \cdot \nabla w \, \mathrm{dV} \tag{19}
$$

where

$$\begin{cases} -\nabla \cdot \left(\frac{1}{\rho(\mathbf{x})} \nabla \phi(\mathbf{x}) \right) = 0 & \text{for } \mathbf{x} \in \Omega \\ \frac{1}{\rho(\mathbf{x})} \nabla \phi(\mathbf{x}) \cdot \mathbf{n} = I(\mathbf{x}) & \text{for } \mathbf{x} \in \partial\Omega. \\ -\nabla \cdot \left(\frac{\nabla w}{\rho(\mathbf{x})} \right) = 0 & \text{for } \mathbf{x} \in \Omega \\ \frac{\nabla w}{\rho(\mathbf{x})} \cdot \mathbf{n} = g(\mathbf{x}) & \text{for } \mathbf{x} \in \partial\Omega \end{cases} \tag{20}$$

These equations will be useful when designing both I and g given some initial assumptions on rho and $\tilde{\rho}$, i.e. we will try to use these equations to design sets of measurements containing a lot of information of the subsurface.

The response for a homogeneous half-space

Let's study our very important special case where the domain of interest is a half-space with a constant resistivity and the injection is made from a single point-source on the edge and the potential reading is made in a single point i.e:

$$\begin{aligned} \Omega &= \left\{ \mathbf{x} = (x, y, z) \in \mathbb{R}^3 | z < 0 \right\} \\ \partial\Omega &= \left\{ \mathbf{x} \in \mathbb{R}^3 | z = 0 \right\} \\ \rho(\mathbf{x}) &= \rho_0 \\ I(\mathbf{x}) &= \delta(\mathbf{x} - \mathbf{x}_c) \\ g(\mathbf{x}) &= \delta(\mathbf{x} - \mathbf{x}_p) \end{aligned}$$

where $\mathbf{x}_c$ and $\mathbf{x}_p$ are assumed to be in the plane $z = 0$. For this case the PDEs in (20) have easy solutions:

$$\begin{aligned} \phi = \phi_c &= \frac{\rho_0}{2\pi |\mathbf{x} - \mathbf{x}_c|} \\ w = \phi_p &= \frac{\rho_0}{2\pi |\mathbf{x} - \mathbf{x}_p|} \end{aligned}$$

this give us:

$$\phi_c(\mathbf{x}) = \frac{\rho}{2\pi |\mathbf{x} - \mathbf{x}_c|} \tag{21}$$

$$\phi_p(\mathbf{x}) = \frac{\rho}{2\pi |\mathbf{x} - \mathbf{x}_p|} \tag{22}$$

and

$$F(\tilde{\phi}) = \int_\Omega \frac{\tilde{\rho}(\mathbf{x})}{4\pi^2 \rho_0^2} \frac{(\mathbf{x} - \mathbf{x}_c) \cdot (\mathbf{x} - \mathbf{x}_p)}{|\mathbf{x} - \mathbf{x}_c|^3 |\mathbf{x} - \mathbf{x}_p|^3} \, \mathrm{dV} \tag{23}$$

which is the response of this measurement to the perturbation $\tilde{\rho}$. This kind of measurement is called a pole-pole measurements since one pole is used for

current injection and one pole is used for a potential reading. This kind of measurement is not possible to make, it violates both the constraints of g and I, but it is very useful as a tool for building solutions to more complex problems.

For a real measurement we use two point sources for current injections and measure the potential difference between two points on the surface. But this case is easy to build with the special pole-pole case discussed above:

$$F_{full} = F_{c1,p1} - F_{c1,p2} - F_{c2,p1} + F_{c2,p2} \tag{24}$$

where $F_{ci,pj}$ is the response of the pole-pole with ci as the current electrode and pj as the potential electrode. The response is still dependent on the basis of perturbation $\tilde{\rho}$ and different choices of $\tilde{\rho}$ will corresponds to different models of the subsurface which we will discuss below.

4.1.1 The 3D sensitivity function of a homogeneous half-space

If we want to model the subsurface in 3D ,i.e. we believe the true resisitivity of the ground can change with any of the spatial dimension, we can choose a $\tilde{\rho}$ that is zero outside a volume element V and 1 inside the volume element.

$$\tilde{\rho}(\mathbf{x}) = \begin{cases} 1 & \text{for } \mathbf{x} \in V \\ 0 & \text{for } \mathbf{x} \notin V \end{cases} \tag{25}$$

the response of a pole-pole measurement will be:

$$F(\tilde{\phi}) = \int_V \frac{1}{4\pi^2\rho_0^2} \frac{(\mathbf{x}-\mathbf{x}_c)\cdot(\mathbf{x}-\mathbf{x}_p)}{|\mathbf{x}-\mathbf{x}_c|^3|\mathbf{x}-\mathbf{x}_p|^3} d\mathbf{x} \tag{26}$$

The *3D-sensitivity* of a measurement is the integrand of this response i.e.

$$J_{3D}(\mathbf{x}) = \frac{1}{4\rho_0^2\pi^2} \frac{(\mathbf{x}-\mathbf{x}_c)\cdot(\mathbf{x}-\mathbf{x}_p)}{|\mathbf{x}-\mathbf{x}_c|^3|\mathbf{x}-\mathbf{x}_p|^3}. \tag{27}$$

The sensitivity can thus be interpreted as the function we need to integrate in order to get the response to a small resisitivity change in the given volume V. This means that we can, at least formally, view this sensitivity function as the response to Dirac perturbation.

4.1.2 The 2D sensitivity function

In many cases the resistivity in the subsurface is assumed to only depend on the x-coordinate and z-coordinate meaning that the resitivity does not change as we travel along the y-axis. In order to mimic this in the perturbation of the resisitivity a perturbation that does not depend on y should be chosen. We use a perturbation on the from:

$$\tilde{\rho}(\mathbf{x}) = \begin{cases} 1 & \text{for } (x,z) \in S \\ 0 & \text{for } (x,z) \notin S \end{cases} \tag{28}$$

The response of a pole-pole measurement for this perturbation is:

$$F(\tilde{\phi}) = \int_S \left(\int_{-\infty}^{\infty} \frac{1}{4\pi^2 \rho_0^2} \frac{(\mathbf{x}-\mathbf{x}_c)\cdot(\mathbf{x}-\mathbf{x}_p)}{|\mathbf{x}-\mathbf{x}_c|^3 |\mathbf{x}-\mathbf{x}_p|^3} \, \mathrm{dy} \right) \mathrm{dx}\, \mathrm{dz}. \tag{29}$$

The 2D-sensitivity is the integrand of the surface integral of the response i.e.

$$J_{2D}(x,z) = \int_{-\infty}^{\infty} \frac{1}{4\pi^2 \rho_0^2} \frac{(\mathbf{x}-\mathbf{x}_c)\cdot(\mathbf{x}-\mathbf{x}_p)}{|\mathbf{x}-\mathbf{x}_c|^3 |\mathbf{x}-\mathbf{x}_p|^3} \, \mathrm{dy},$$

which we can formally interpret as the response of pole-pole measurement to a small resitivity change in a line parallel to the y-axis located at (x,z).

When $\mathbf{x}_c = (x_c, y_0, 0)$ and $\mathbf{x}_p = (x_p, y_0, 0)$, i.e the potential pole and the current pole are on the same y-coordinate, this integral has a solution given by complete elliptic integrals of the first, denoted K, and second, denoted E, kind. The result, with a slight change of notation in order to be consistent with previous results, is only presented here— the full derivation is found in [3]:

$$J_{2D}(x,z) = \frac{1}{2\pi^2 \rho_0^2 \alpha \beta^2} \left(\frac{\alpha^2 E(k) - \beta^2 K(k)}{(\alpha^2 - \beta^2)} - \gamma \frac{\left(\alpha^2 + \beta^2\right) E(k) - 2\beta^2 K(k)}{\left(\alpha^2 - \beta^2\right)^2} \right) \tag{30}$$

where

$$k = \frac{\left(\alpha^2 - \beta^2\right)^{\frac{1}{2}}}{\alpha} \tag{31}$$

and

$$\alpha^2 = (x - x_c)^2 + z^2 \tag{32}$$
$$\beta^2 = (x - x_p)^2 + z^2 \tag{33}$$
$$\gamma = (x - x_c)(x_p - x_c) \tag{34}$$
$$\tag{35}$$

for $x > 0.5(x_c + x_p)$ and

$$\alpha^2 = (x - x_p)^2 + z^2 \tag{36}$$
$$\beta^2 = (x - x_c)^2 + z^2 \tag{37}$$
$$\gamma = (x_p - x_c)(x_p - x) \tag{38}$$
$$\tag{39}$$

for $x < 0.5(x_c + x_p)$ and

$$\alpha^2 = 0.25\,(x_p - x_c)^2 + z^2 \tag{40}$$
$$J_{2D}(x,z) = \frac{1}{4\pi} \left(\frac{1}{2\alpha^3} - \frac{3a^2}{16\alpha^5} \right) \tag{41}$$

for $x = 0.5(x_c + x_p)$.

This is the sensitivity that will be primarily discussed in this report but the methods discussed should be general enough that it should be easy to switch the dimension of the sensitivity.

4.1.3 The 1D sensitivity function

If we instead believe that the subsurface is made out of layers using a perturbation that only depends on the depth makes sense, we can write such a perturbation as:

$$\tilde{\rho}(\mathbf{x}) = \begin{cases} 1 & \text{for } z \in I_z \\ 0 & \text{for } z \notin I_z \end{cases} \tag{42}$$

The response of a pole-pole measurement for this perturbation is:

$$F(\tilde{\phi}) = \int_{I_z} \left(\int_{-\infty}^{\infty} \int_{-\infty}^{\infty} \frac{1}{4\pi^2 \rho_0^2} \frac{(\mathbf{x} - \mathbf{x}_c) \cdot (\mathbf{x} - \mathbf{x}_p)}{|\mathbf{x} - \mathbf{x}_c|^3 |\mathbf{x} - \mathbf{x}_p|^3} \, \mathrm{dx}\, \mathrm{dy} \right) \mathrm{dz}. \tag{43}$$

The 1D-sensitivity is the integrand of the z-integral of the response i.e.

$$J_{1D}(z) = \int_{-\infty}^{\infty} \int_{-\infty}^{\infty} \frac{1}{4\pi^2 \rho_0^2} \frac{(\mathbf{x} - \mathbf{x}_c) \cdot (\mathbf{x} - \mathbf{x}_p)}{|\mathbf{x} - \mathbf{x}_c|^3 |\mathbf{x} - \mathbf{x}_p|^3} \, \mathrm{dx}\, \mathrm{dy},$$

which we can formally interpret as the response of pole-pole measurement to a small resitivity change in a plane orthogonal to the z-axis located at depth z. This integral has a solution:

$$J_{1D}(z) = \frac{2}{\pi} \frac{z}{\left(|\mathbf{x}_c - \mathbf{x}_p|^2 + z^2 \right)^{\frac{3}{2}}} \tag{44}$$

4.2 Geometrical factor

When taking a measurement on a half-space the apparent resisitivity value can be calculated as:

$$\rho_a = k \frac{\phi}{I} \tag{45}$$

$$k = \frac{2\pi}{\left(\frac{1}{r_{C_1 P_1}} - \frac{1}{r_{C_1 P_2}} - \frac{1}{r_{C_2 P_1}} + \frac{1}{r_{C_2 P_2}} \right)}. \tag{46}$$

where I is the current, ϕ is the measured potential, and $r_{C_i P_j}$ is the euclidean distance from the current electrode C_i and the potential electrode P_j [1]. Note that the geometrical factor, denoted k, is only dependent on the position of the electrodes and not the measured potential or the injected current.

If the subsurface is indeed homogeneous then ρ_a is the correct resistivity of the subsurface. In this case we can see that measurements with high geometric factor are inferior to the measurements with lower geometric factor — any noise present in the potential measurements will be scaled with the geometric factor. Assuming Gaussian white noise added to the potential measurement we would get:

$$\hat{\rho}_a = k\frac{\phi + \epsilon}{I} \tag{47}$$

$$\epsilon \in N(0, \sigma), \tag{48}$$

but this is easily rewritten as:

$$\hat{\rho}_a = k\frac{\phi}{I} + k\frac{\epsilon}{I} = \rho_a + k\frac{\epsilon}{I} \in N\left(\rho_a, \left|\frac{k}{I}\right|\sigma\right). \tag{49}$$

This shows that higher geometric factors will lead to measurements with higher standard deviation compared to measurements with lower geometric factor.

We can also take another viewpoint — the measured potential, should the subsurface really be homogeneous, will be lower if the geometric factor is larger compared to a measurement with smaller geometric factor. This would again lead to worse signal-to-noise ratio if the noise is assumed to be independent from the measured potential. The geometrical factor is thus important because it gives a hint of the noise performance of the measurement, later we will use the geometric factor for pre-processing — we will not consider measurements with very high geometric factor. The removal of measurements with high geometric factor is also done in previous research [9] [8].

4.3 The tomographic or inversion problem

Once a set of measurements along the boundary of some domain Ω have been made, the resistivity distribution $\rho(\mathbf{x})$ over Ω can be estimated. This is usually called the 'Inversion problem' [1]. One method, and the one used in this paper, is to parameterize a model of the resistivity:

$$\rho(\mathbf{x}) = \rho(\mathbf{x}, \beta)$$

and then look at the squared residuals:

$$r_i = \left(\rho_i^a - F_i(\rho(\mathbf{x}, \beta))\right)^2$$

where ρ_i^a is the apparant resistivity of measurement i and F_i is a forward model for measurement numbered i i.e what would the measured apparent resistivity be if the true resistivity is $\rho(\mathbf{x}, \beta)$. The idea is to minimize the sum of r_i by changing β. Typical choices of β is to split the ground in to blocks and assuming that the resistivity is constant within the blocks. This section is only meant to give the reader the general idea of how inversion is done, for a full description

refer to [1] [6].

4.4 Number of possible measurements and different kinds of measurements

A single measurement is just a selection of 4 electrodes out of the N electrodes available to the instrument. Each selection of 4 electrodes can be arranged in 3 non-equivalent, from an electrical perspective, ways. The equivalence of some 4 electrode arrangements is easily seen:

1. Switching P1 and P2 will only switch the sign of the resulting measurement.
2. Switching C1 and C2 will only switch the sign of the resulting measurement.
3. Switching P1 and C1 and at the same time switching C2 and P2 will result in the same measurements. Switching in this way gives the 'reciprocal' measurements which are useful for testing data-quality [1].

There are a total 24 ways to assign C1,C2,P1,P2 to 4 electrodes — but each entry in the list above will remove half of the remaining permutations leading to $\frac{24}{8} = 3$ non-equivalent ways of assigning the electrodes.

This means that for a electrode layout of N electrodes there are:

$$N_{meas} = \frac{N!}{(N-4)!4!} \cdot 3 = \frac{N(N-1)(N-2)(N-3)}{8} \tag{50}$$

non-equivalent arrays.

In practice it is common to fixate the role of an electrode as either a potential electrode or as a current electrode meaning that it can only assume one of these roles in measurements. This is done for two reasons:

1. It completely removes the problem of polarization associated with using an electrode as a potential electrode to soon after using it as a current electrode. [1] [8]
2. It makes acquiring the reciprocal measurements easier as the roles of the electrodes can be easily switched and the same measurements taken again.

Using this kind of setup will also naturally shrink the number of possible measurements. With N_c current electrodes and N_p potential electrodes the total number of measurements is:

$$N_{meas} = \frac{N_c!}{(N_c-2)!2!} \frac{N_p!}{(N_p-2)!2!} = \frac{N_c(N_c-1)N_p(N_p-1)}{4}. \tag{51}$$

The different types of measurements can be divided in to 3 classes, assuming the electrodes are laid on a line, based on the arrangement of the electrodes. The different classes are:

1. α-arrays: The electrodes are arranged C1-P1-P2-C2
2. β-arrays: The electrodes are arranged C1-C2-P1-P2
3. γ-arrays: The electrodes are arranged C1-P1-C2-P2

arrangements that are equivalent according to the previous list is also considered part of the corresponding class.

4.5 Previous research

Most previous research rely on building a block model of the subsurface and calculating the sensitivity with regards to a change in resisitivty within each block. These methods usually also calculate the resolution matrix and use this to find a suitable set of measurements to take [9] [8] [4]. The methods discussed here are only based on sampling the sensitivity function over some region. Methods based on the resolution matrix requires a inversion of a large matrix — however the use of parallell computation via GPUs and clever optimization of the running time has made latest version of the 'Compare R' algorithm is fairly fast [4]. Versions of the 'Compare R' algorithm for multichannel measurements do exist but will fail to fully use the multichannel capabilities of the terrameter, as will be discussed later. Multichannel versions of 'Compare R' rely on building a sequence of measurements with the same current electrodes but changing one of the potential electrodes, making a chain of potential electrodes to measure between [8].

5 Theory

5.1 Notation

Before rushing of into solving different optimization problems it is important to fixate notation and language use. The sensitivity of a measurement indexed i will be denoted J_i. The sensitivity can in general be thought of as arising from a general domain Ω, but in practise only the $2D$-senstivity of a homogeneous halfspace was tested, evaluated and used. For a set of measurements we will denote their cumulative absolute sensitivity as:

$$\hat{J}_I(\mathbf{x}) = \sum_{i \in I} |J_i(\mathbf{x})| \,. \tag{52}$$

In practice it is also necessary to discretizes the model. In this paper J will also, depending on context, denote a matrix with elements $J_{i,j} = J_i(\mathbf{x}_j)$ where

$\mathbf{x}_j$ is the j:th discretization point. This matrix is of interest mainly for the implementation and will only be used when implementation is discussed. The size of J is $N \times M$ where N is the number of all considered measurements and M is the number of discretization points.

For all of the methods discussed it is reasonable to select a *domain of interest*, denoted A, which is the subset of Ω (as presented in section 4.1) we are interested in modelling — we are after all not interested in , for instance, all of the subsurface but rather only the part close to the placed electrodes and down to some pre-determined depth. For practical purposes the top-strip of the subsurface should be excluded from the domain of interest due to the numerical properties of sensitivities close to the electrode positions. The set of all considered measurements is called the *comprehensive set* in order to mimic the language used in previous research.

5.2 Problem description, mathematical formulation

Now that we have the fundamental entities in place it is time to formulate the problem of selecting the optimal set of measurements to make as a mathematical problem. In general areas of high absolute sensitivity are fairly well resolved, but they can only give a true indication of real-world performance in limited cases [9] — i.e. the model resolution and the sensitivity are *connected*, but they are *not* the same thing. Still the idea of summing the absolute sensitivity functions has intuitive appeal — we want to increase the response we get from a resistivity change so it makes sense to maximise the sensitivity in some sense. The main problem is that the sensitivity in general is a function over as many as three dimensions, and in order to optimize we would need to boil this down to a single number representing how good the sensitivity pattern of a given set of measurements is. A further issue is that the sensitivity pattern of a full set might not give a full indication of its performance when inverting a real data set due to heavy overlap between measurements — meaning that some measurement add very little information of the subsurface, given the other measurements, even though they have high sensitivity — this can be exemplified by having a set full of repeating (noise free) measurements, the sensitivity of this set increases with the set's size but the expected performance is the same as all measurement contain the same information.

We will however try different methods of optimization in order to find 'optimal' sets of measurements, we begin with a general description in mathematical terms.

5.3 Formulation as an optimization problem

Let $J_i(\mathbf{x})$ denote the sensitivity function of measurement numbered i and let F be a functional from the space of sets of continuous functions to the real numbers. Note that the kind of sensitivity function $J_i(\mathbf{x})$ denotes depend on

the dimension of $\mathbf{x}$. The optimization problem becomes:

$$\begin{gathered} \max_I F\left(\{J_i(\mathbf{x})\}_{i\in I}\right) \\ \text{such that} \\ |I| = N. \\ I \subset I_{all} \end{gathered} \tag{53}$$

where I_{all} denotes the set of all indices of the considered measurements. In plain text: find a set containing N entries from the set of all measurements such that the functional applied to the sensitivities of the selected set attain a maximum value.

As the number of measurements is bounded, it is easy to see that the problem in (53) has at least one solution and it can be found by simply studying all the subsets of I_{all} of size N, evaluating the functional and selecting the subset with the highest value. This is in general not feasible however as the number of subsets of size N will be *very* large.

6 Considered methods

The problem formulation in section 5.2 is only useful once an appropriate F has been determined. How F is chosen will have a dramatic impact on the resulting sensitivity pattern, and while each one might maximize some metric of the 'goodness' of the sensitivity it might falter in many other regards. In this section a couple of different F will be studied.

There are also methods which do not correspond directly to an intuitive goal-function but rather aim to build a sensitivity pattern that has the features we want it to with some heuristic. Both of these angles will be discussed in this section. In 5.2 there was no special attention to the use of the multichannel capabilities of the measurement system — this would have to be incorporated into the goal-function. This is a daunting task however and the methods optimized for multichannel use will fall in the second category of methods, without a clear goal-function.

6.1 The integral or sum as a goalfunctions

An easy way of assigning a value for each measurement set is to study the integral of the sum of absolute sensitivities of the measurements in that set over the domain of interest. This would mean that

$$F(y) = \int_A y(\mathbf{x})w(\mathbf{x})d\mathbf{x}, \tag{54}$$

where A is the domain of interest, in the continuous case and

$$y = \sum_{i \in I} |J_i(\mathbf{x})| \tag{55}$$

and $w(\mathbf{x})$ is a weight function. Intuitive choices of weight functions are either $w(\mathbf{x}) = 1$ and $w(\mathbf{x}) = \left(\sum_{i \in I_{all}} |J_i(\mathbf{x})|\right)^{-1}$.

This version of F, while simple, might not perform in a satisfactory way. It does not, for instance, in any way try to spread out the measurements so that we get a nice coverage of all of the domain instead it only cares about the total sensitivity. As such it is likely to select a set of measurements looking very similar to one another in terms of sensitivity. The method does have the nice property of the optimum being very easy to compute — all one needs to do is to calculate the integral of each measurement by some numerical integration method and pick the N measurements with the highest integral. The numerical integration was done with the trapezoidal method, for evenly spaced sample points the direct sum rescaled with the area between the sample points could also be used in order to get a very fast method. This method is *not* expected to perform particularly well, it is mostly include as a baseline to gauge the performance of other methods.

6.2 Spread of center of mass

The previous goal-function aim at having a high average sensitivity or a high average sensitivity when weighed with the full set. The method presented in this section instead focus on spreading the total sensitivity evenly across the subsurface. This method calculates the centre of mass for every measurement, and use this as a 'location' of the measurement. We then want to find a set of measurement such that the measurements are far from each other. After the center of mass has been calculated for each measurement the problem can be formulated as a optimization problem:

$$\begin{gathered} \max_I d(I) \\ \text{such that} \\ |I| = N. \\ I \subset I_{all} \end{gathered} \tag{56}$$

where

$$\begin{gathered} d(I) = \min_{\mathbf{x},\mathbf{y} \in I} \|\mathbf{x} - \mathbf{y}\| \\ \text{such that} \\ \mathbf{x} \neq \mathbf{y} \end{gathered} \tag{57}$$

i.e. d is the minimum distance between two points in the set I. The optimization problem is to find the subset of I_{all} of size N with the maximum smallest

distance between two points in the subset. The full optimization problem, going directly from the sensitivities is:

$$\max_{I} d\left(\left\{\frac{1}{\int_{\Omega}|J_i(\mathbf{x})|d\mathbf{x}}\int_{\Omega}|J_i(\mathbf{x})|\cdot\mathbf{x}d\mathbf{x}\right\}_{i\in I}\right) \quad \text{such that} \quad |I|=N \quad I\subset I_{all}, \tag{58}$$

which again follows the format of 5.2, but with a more complicated goal-function F.

Note that the center of mass is only one possible way to map a measurement to a point in some multidimensional space — we could imagining assigning each measurement to a much longer 'feature' vector, and the same general idea could be used. Using a longer feature vector with the same general idea would mean that we emphasize selecting as different measurements as possible. Using the mass centers as features vector does however simplify visual representation and it should be relativly close to the location of the pseudosection data points used for initial plotting of field data, giving it a nice interpretation.

In order to find a good candidate solution for (56) an initial set of measurements is selected in some way, for instance the measurement closest to the center of mass of all measurements. After this the following procedure is used:

1. Calculate the *shortest* distance from every measurements centre of mass to the so far chosen set. The shortest distance is the distance to the nearest point in the selected set.
2. Sort the distance and select a number of measurements with the maximum shortest distance to the set. Add these to the set.
3. Iterate until enough measurements have been chosen.

This is a extremely simple, and not particularly computationally intensive method of choosing sets, it will probably not however yield an optimal solution to (56). The resulting set will usually have pretty low cumulative sensitivity, but the ratio of the cumulative sensitivity with the sensitivity of the full set is very smooth — indicating that the set has the same relative sensitivity to the different areas of the subsurface as the full set.

6.3 Correlation

The method discussed in 6.2 tries to spread samples evenly across a metric feature space, instead this method tries to find measurements that in some

sense has a large 'angle' between them. In order to introduce the concept of angles between measurement we will need an inner product to work with. The absolute sensitivity functions are all square integrable if the top strip of the subsurface is excluded to avoid problems with the sensitivity extremely close to the electrodes. Thus a reasonable inner product to choose is the $L_2(A)$ inner-product:

$$\begin{aligned} \langle f, g \rangle &= \int_A f(\mathbf{x}) g(\mathbf{x}) \, \mathrm{d}\mathbf{x} \\ \|f\|^2 &= \int_A f(\mathbf{x})^2 \, \mathrm{d}\mathbf{x} \end{aligned} \tag{59}$$

We want to have a measure of how large the angle between 2 measurements is — to do this it is reasonable to study the value:

$$C(f, g) = \left(\frac{\langle f, g \rangle}{\|f\| \cdot \|g\|} \right).$$

The normalization is there to make the estimate invariant with scaling, and if f and g are thought of as vectors in $\mathbf{R}^n$ with the normal inner product the value could be interpreted as cosinus of the smallest angle between the vectors.

The value $C(f, g)$ is an estimate of how large the angle between f and g are, due to the normalization with the norm it is invariant when scaled with a constant but *adding* a constant to f or g will give different results. In order to get a value invariant to the addition of a constant we can subtract the mean of f and g respectively.

$$C_2(f, g) = C(f - m_f, g - m_g) = \left(\frac{\langle f - m_f, g - m_g \rangle}{\|f - m_f\| \cdot \|g - m_g\|} \right) \tag{60}$$

where m_f and m_g are the average value of f and g. Now we have a measure of similarity that is both invariant with scaling and with addition of a constant.

With these tools in place we are ready to formulate a optimization problem similar to the one found in section 6.2 but the function $d(\cdot)$ has changed. We could look at the problem of

$$\begin{gathered} \min_I d_2(I) \\ \text{such that} \\ |I| = N. \\ I \subset I_{all} \end{gathered} \tag{61}$$

where

$$\begin{gathered} d_2(I) = \max_{f,g \in I} C_2(f, g) \\ \text{such that} \\ f \neq g \end{gathered} \tag{62}$$

The problem in (61) can be summarized as finding the set measurement of size N where the largest similarity between two entries, measured with C_2, is as small as possible. In order to use this problem directly for the problem of selecting measurements we can take I_{all} as the set of all the measurements' absolute sensitivity functions.

The function C_2 is defined by integrals, but it will need to be evaluated often for many different f and g. Instead of calculating the integrals with highly accurate numerical integration methods, a rectangle integration scheme can be used. We approximate:

$$C_2(f,g) \approx \frac{\sum_j A_j \left(f(\mathbf{x}_j) - m_f\right)\left(g(\mathbf{x}_j) - m_g\right)}{\sqrt{\sum_j A_j \left(f(\mathbf{x}_j) - m_f\right)^2 \cdot \sum_j A_j \left(g(\mathbf{x}_j) - m_g\right)^2}} \tag{63}$$

where A_j is the area of the j:th sample points associated rectangle and $f(\mathbf{x}_j)$ denote the sample points. Assuming that the samples are equally spaced i.e $A_j = A_0$ for all j we can move the area scaling outside of the sum, at which point it cancels, and the result is:

$$C_2(f,g) \approx \frac{\sum_j \left(f(\mathbf{x}_j) - m_f\right)\left(g(\mathbf{x}_j) - m_g\right)}{\sqrt{\sum_j \left(f(\mathbf{x}_j) - m_f\right)^2 \cdot \sum_j \left(g(\mathbf{x}_j) - m_g\right)^2}} \tag{64}$$

which is identified as the Pearson correlation between two elements in I sampled at the points $\mathbf{x}_j$. This means that we could view the sample points of the sensitivity functions for the different measurements as samples of a stochastic variable, comparing two measurements by their correlation. The problem in (61) can then by summarized as finding the set measurement of size N such that the largest correlation between two measurements' sampled absolute sensitivity functions is as small as possible.

In order to get a close to optimum solution to problem (61) the following local optimization algorithm is used:

1. Select an initial set of measurements consisting of the dipole-measurements.
2. Calculate the maximum correlation for all non-selected measurements.
3. Sort the maximum correlations and select the n measurements with the lowest maximum correlation. Add these to the set.
4. Iterate 2-3 until enough measurements have been chosen.

We have no guarantee that the proposed algorithm should find the correct optimum however and it seems unlikely that it should. The idea is to get something close enough, with the general property that the measurements have low correlation to one another.

7 Multichannel measurements

The main goal of this article is to optimize the measurement sets also for mulitchannel use — the methods discussed above are mostly used for comparison and as building blocks for these methods. This section is dedicated to discussing how the multichannel system works and how measurement sets can be designed to use it full potential.

The properties of the considered terrameter and a simplified model

The 'ABEM Terrameter LS 2' has the capabilities of making more than one potential reading at a time i.e. for a given pair of current electrodes we measure the potential between more than one pair of potential electrodes. The instrument has 12 channels in total, but all of these cannot be used at the same time except in specific circumstances. A simple model of the switchboard is shown in figure 3.

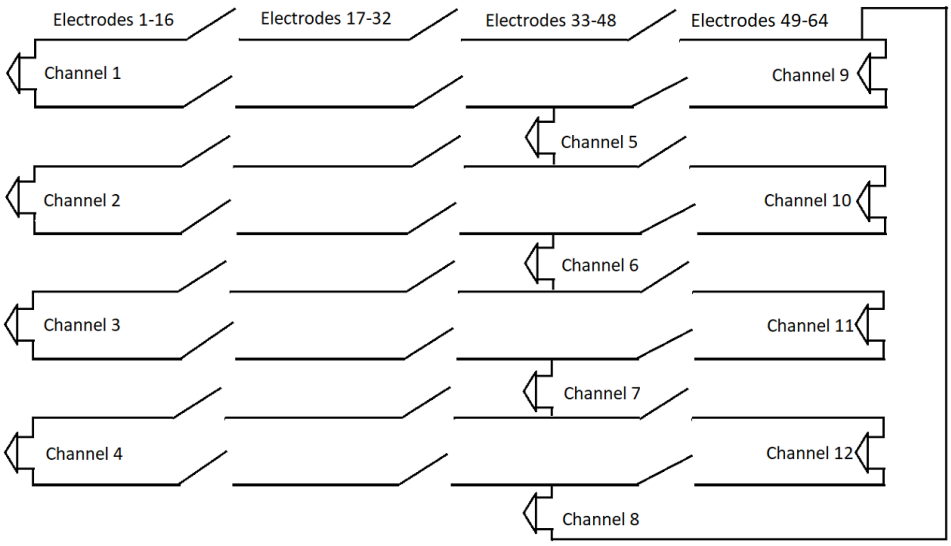

Figure 2: A diagram of the switchboard of the 'ABEM Terrameter LS 2'. The horizontal lines have access to the electrodes used for the survey. Lets first assume that all the switches are opened — this divides the lines into segments with each segment having access to 16 electrodes. Each of these segments can be assigned one of the electrodes it has access to. A channel is just a connection between two segments representing a potential reading between the electrodes assigned to the different segments. This means that channel 1 can make a potential reading between two electrodes numbered 1 to 16 (assuming still that all the switches are opened). When a switch is closed the segments are merged, e.g. by closing the first switch on the first line channel 1 could make a measurement with one electrode numbered between 1 and 32 and one between 1 and 16. By also closing the two first switches on the second line the second electrode of the first channel would necessarily be the same as the the first electrode on channel 5 since they are connected to the same merged segment. Note in particular that channel 8 connects to the last segment of the first line, making it special both because it connects to two different sets of electrodes (if the switches are opened) and because it loops around to the first line.

The model can also be presented as a table as shown in 1.

Line	Electrode $1-16$		Electrode $17-32$		Electrode $33-48$		Electrode $49-64$
1	CH_1 P_1	switch		switch		switch	CH_8 P_2, CH_9 P_1
2	CH_1 P_2	switch		switch	CH_5 P_1	switch	CH_9 P_2
3	CH_2 P_1	switch		switch	CH_5 P_2	switch	CH_{10} P_1
4	CH_2 P_2	switch		switch	CH_6 P_1	switch	CH_{10} P_2
5	CH_3 P_1	switch		switch	CH_6 P_2	switch	CH_{11} P_1
6	CH_3 P_2	switch		switch	CH_7 P_1	switch	CH_{11} P_2
7	CH_4 P_1	switch		switch	CH_7 P_2	switch	CH_{12} P_1
8	CH_4 P_2	switch		switch	CH_8 P_1	switch	CH_{12} P_2

Table 1: There are a total of 12 channels labeled $CH_1 - CH_{12}$. Each channel can make one potential reading between two electrodes for a given pair of current injecting electrodes. Each channel thus needs to be connected to two potential electrodes P_1 and P_2 respectively. By default the channels only have access to the electrodes they are directly connected to e.g. Channel 1 can make a potential reading between two electrodes numbered $1-16$ and channel 8 can make a potential reading from an electrode numbered $33-48$ and an electrode numbered $49-64$. By closing the switches more electrodes can be accessed by the channels but channels connected by lowered switches would have to have the same electrode. For instance by lowering all switches on line 3 and line 4 channel 2 and channel 10 would make the same measurement, channel 5 and channel 6 would by necessity share a potential electrode with these two measurements.

By default each channel only has access to the parts of the line it is directly connected to. By lowering the switches a channel can be given access to more electrodes. By lowering *all* the switches a total of 8 measurements can be produced as long as the measurements share electrodes in a chain. This is the idea behind the modified 'Compare R' algorithm in [8], this will however mean that a maximum of 8 out of the 12 channels can be used at each current injection.

Instead of lowering all the switches we can retain the capabilities of making 12 measurements by not lowering a few selected switches. This simplification of the switchboard is shown below.

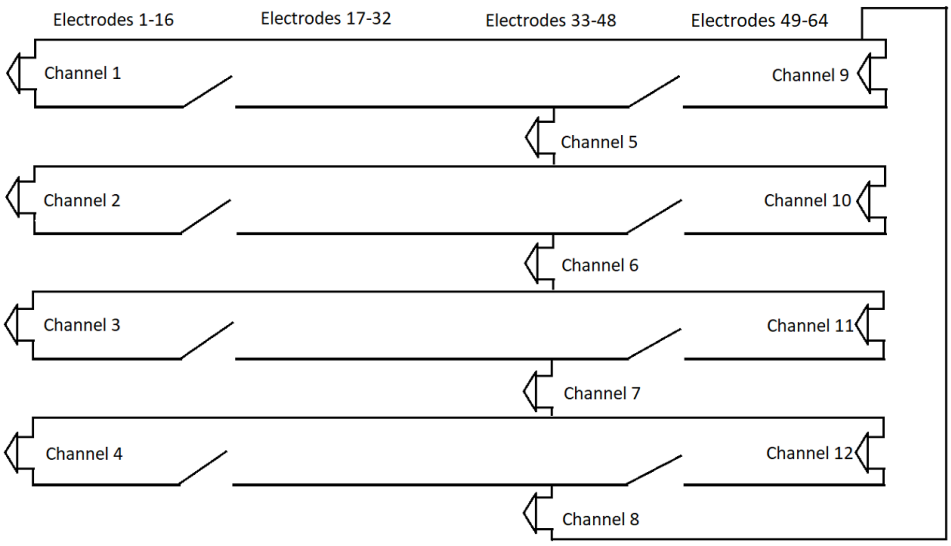

Figure 3: A diagram of the simplified switchboard. The open switches are connected in the sense that one of them is always open while the other is closed. This means that only a total of 12 electrodes can be chosen, while the original board in theory can allocate 23 electrodes. Note in particular that the lines 1, 3, 5 and 7 are now fully connected and has access to all different electrodes from $1-64$, all the channels connected to these lines hence have to share at least one electrode.

The reasoning behind this simplification is that we remove some asymmetries in the original switchboard. Channel 8 was previously a special channel because it was connected to the last segment of the first line but in this simplification that does not matter because all switches on the first line is lowered. This makes channel 8 directly comparable to channel 5, 6 and 7. Furthermore, the closing of the middle switches makes the board symmetric when flipping the board left-right. We can present the same simplification as a table:

Line	Electrode $1-16$		Electrode $17-32$		Electrode $33-48$		Electrode $49-64$
1	CH_1 P_1	closed		closed		closed	CH_8 P_2, CH_9 P_1
2	CH_1 P_2	switch		closed	CH_5 P_1	switch	CH_9 P_2
3	CH_2 P_1	closed		closed	CH_5 P_2	closed	CH_{10} P_1
4	CH_2 P_2	switch		closed	CH_6 P_1	switch	CH_{10} P_2
5	CH_3 P_1	closed		closed	CH_6 P_2	closed	CH_{11} P_1
6	CH_3 P_2	switch		closed	CH_7 P_1	switch	CH_{11} P_2
7	CH_4 P_1	closed		closed	CH_7 P_2	closed	CH_{12} P_1
8	CH_4 P_2	switch		closed	CH_8 P_1	switch	CH_{12} P_2

Table 2: The switches marked 'closed' are now permanently closed reducing the switchboards degrees of freedom drastically. The switches left are also connected in the sense that one of them is always open while the other is closed. This means that only a total of 12 electrodes can be chosen, while the original board in theory can allocate 23 electrodes. Note in particular that the lines 1, 3, 5 and 7 are now fully connected and has access to all different electrodes from $1-64$, all the channels connected to these lines hence have to share at least one electrode.

In the simplfied switchboard we close a couple of the switches, sacrificing degrees of freedom on the board in favour of a more easily modeled board. In order to avoid taking duplicate measurements the switches that on the same row can not be close nor open at the same time — each of these lines will have one open and one closed switch. This simplified switchboard also has a couple of interesting features—it is circularly symmetrical if it is rotate up-down by two rows, this due to the closed switches on the first line making the fact that the second potential electrode of channel 8 is in the last section unimportant. Furthermore it is also right-left symmetric. This can be taken advantage of when designing algorithms for selecting which measurements to take. Due to the closed switches the electrodes used by each of the channels are connected as in the table below:

Line	Electrode		Electrode		Electrode
1	CH_1 P_1	=	CH_8 P_2	and	CH_9 P_1
2	CH_5 P_1	=	CH_1 P_2	or	CH_9 P_2
3	CH_2 P_1	=	CH_5 P_2	and	CH_{10} P_1
4	CH_6 P_1	=	CH_2 P_2	or	CH_{10} P_2
5	CH_3 P_1	=	CH_6 P_2	and	CH_{11} P_1
6	CH_7 P_1	=	CH_3 P_2	or	CH_{11} P_2
7	CH_4 P_1	=	CH_7 P_2	and	CH_{12} P_1
8	CH_8 P_1	=	CH_4 P_2	or	CH_{12} P_2

Table 3: This is a table of which electrodes are equal to each other on the simplified switchboard. Again we see that the lines 1, 3, 4 and 7 have the same electrode all the way through while on the lines 2,4, 6, and 8 the middle channel will share its electrode with either one of the other channels on these lines.

The electrodes allocated to line 1, 3, 5 and 7 will be referred to as *line electrodes*. These are all assumed to be different for a given allocation to the

board. The lines 2, 4, 6, 8 has two different switches on them. The switches on a line can only be closed one at a time i.e. if the first switch is open then the other one is closed and vice versa. This will ensure that we do not get two identical measurements and will make the overall optimization much easier. The state of all the switches on the simplified board can be thus represented as a binary number of length 4, a 1 would mean that the first switch is open and the other is closed and a 0 would mean that the second switch is open and the other is closed. In total there are thus 16 different combinations of switch-positions for the entire simplified switchboard. The electrodes allocated on lines 2, 4, 6 and 8 that are connected to both of their neighbouring line electrodes will be called *link electrodes*. Lastly the electrodes connected to lines 2, 4, 6, 8 without connecting to the next line electrode will be called *leaf electrodes*. In figure 4 the different kinds of electrodes are shown in a graph where a connection represents a measurement between the connected electrodes.

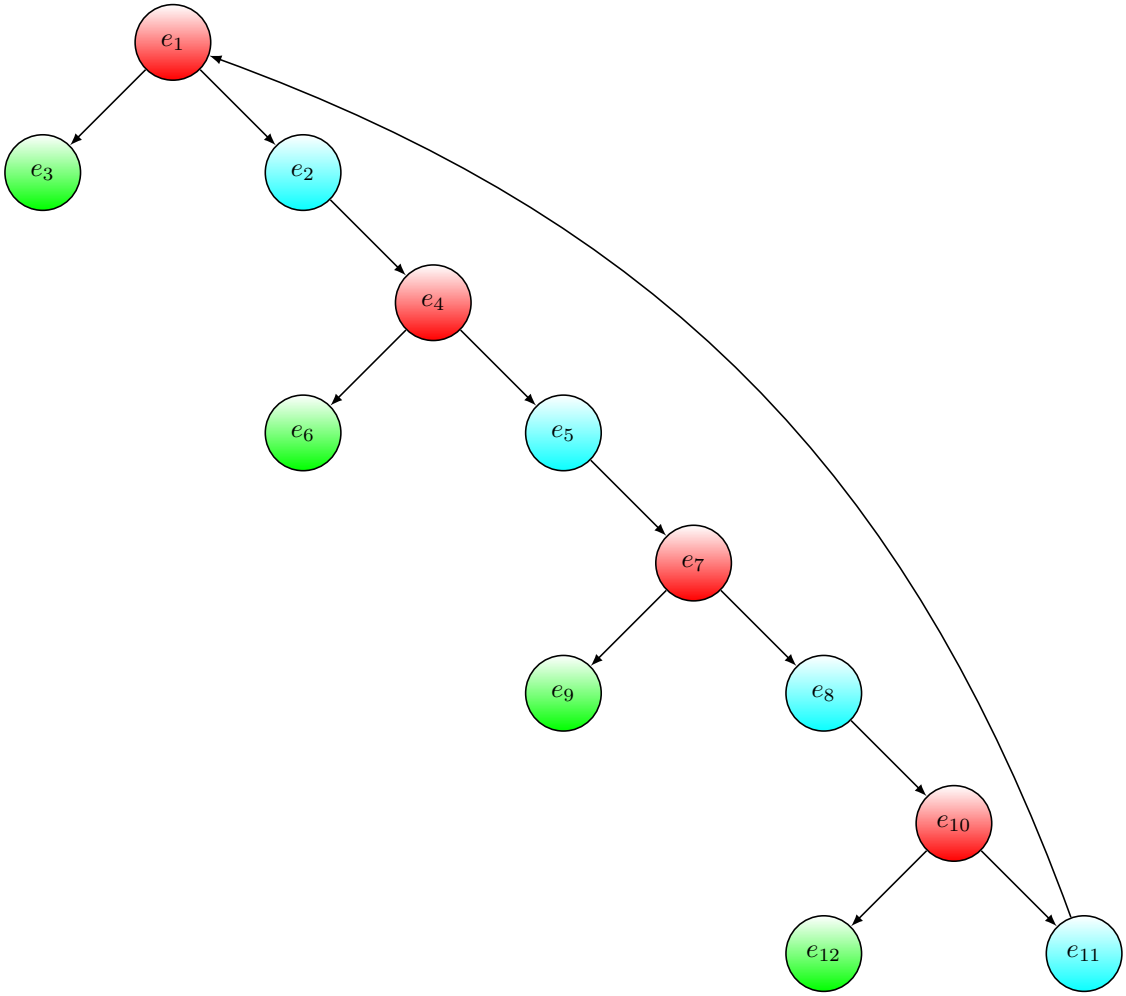

Figure 4: This is a graph of how the different electrodes are connected on the switchboard. The nodes are electrodes and an edge represent a potential measurement between the two connected electrodes, remember that the current electrodes are already given — these are just the different potential electrodes to pair up with the selected current pair. The red nodes are the line electrodes, i.e. the electrodes allocated to the full lines in the simplified switchboard. The blue nodes are link electrodes, i.e. the electrodes that are used for measurements with both of the neighbouring line electrodes. The green nodes represent the leaf electrodes i.e. electrodes which are only used in one measurement with a line electrode. If *all* switches would be closed the green electrodes would be removed from the graph.

The original switchboard has more degrees of freedom as the switches on it can all be operated independently. As each switch position could be represented

by a binary number the state of entire original switchboard could be represented as a binary number of length 24 meaning that there are approximately 10^{23} different states of the original board. Which of course is not feasible to explore by brute force. The total number of states is probably much lower than this for the original switchboard however as some of the states should be equivalent in some sense. The problem does however become much harder to model and implement as the original switchboard is neither circular symmetric or right-left symmetric.

Formulation as an optimization problem

Now that we have briefly discussed the capabilities of the multichannel instrument the question is how to select a set of measurements that fit the instrument and at the same time is 'good' in some sense. How we rank the goodness of a measurement is of course a bit tricky — but we have some ideas from the previously discussed methods of optimizing measurement sets. Assume that every measurement is given a score denoted $S(e_i, e_j)$, representing how good a measurement with the given current pair and e_i and e_j as potential electrodes is. Further assume that the score is additive— the score of a set of measurements is just the sum of the score. Then to maximize the sum of scores gained from an allocation on the switchboard would be the same as finding the allocation with the highest performance. This can be formalized as a unwieldy optimization

problem:

$$
\begin{aligned}
\max \sum_{i\in\{1,4,7,10\}} & S(e_i, e_{i+1}) + S(e_i, e_{i+2}) + S(e_i, e_{c(i-2)}) \\
& \text{such that} \\
1 \leq & e_i \leq 64 \\
1 + 16s_{\lceil \frac{i}{3} \rceil} \leq & e_{i+1} \leq 48 + 16s_{\lceil \frac{i}{3} \rceil} \\
49 - 48s_{\lceil \frac{i}{3} \rceil} \leq & e_{i+2} \leq 64 - 48s_{\lceil \frac{i}{3} \rceil} \\
& e_j \neq e_{j+1} \\
& e_j \neq e_{c(j+2)} \\
& e_j \neq e_{c(j+3)} \\
& e_k \neq e_{c(k-4)} \\
& I(e_l = e_{l+6})I(e_{l+2} = e_{l+8}) = 0 \\
& I(e_l = e_{l+6})I(e_{l+2} = e_{l+7}) = 0 \\
& I(e_l = e_{l+6})I(e_{l+2} = e_{l+4}) = 0 \\
& I(e_l = e_{l+6})I(e_{l+1} = e_{l+8}) = 0 \\
& I(e_l = e_{l+6})I(e_{l+1} = e_{l+7}) = 0 \\
& I(e_l = e_{l+6})I(e_{c(l-2)} = e_{l+8}) = 0 \\
& I(e_l = e_{l+6})I(e_{c(l-2)} = e_{l+4}) = 0 \\
& i \in \{1, 4, 7, 10\} \\
& j \in \{1, 2, 4, 5, 7, 8, 10, 11\} \\
& k \in \{3, 6, 9, 12\} \\
& l \in \{1, 4\} \\
& e_j \in \mathbb{N} \\
& e_k \in \mathbb{N} \\
& s_{\lceil \frac{i}{3} \rceil} \in \{0, 1\} \\
& c(i) = \mod (i-1, 12) + 1
\end{aligned}
\tag{65}
$$

where I is an identiy function returning 1 if the statement is true and 0 if it is false. This optimization problem is the same as looking for graphs as in figure 4 where we give each edge a weight according to the score of that measurement. This optimization problem is for finding the graph with the highest sum of the edges. The inequality conditions makes sure that the measurements are allocatable on the board while the conditions of non-equality and the equality constraints ensures that no repeated measurements are taken and that measurements are between two different electrodes. This formulation is only useful for up to 64 electrodes and for larger layouts special considerations, not discussed here, must be taken, since the switchboard simplification is based partially on the number of electrodes being less than or equal to 64.

The optimization problem presented in equation (65) only deals with how to select a set of potential measurements once a pair of electrodes for current injection has been chosen. One approach is to select which current pair to use by some heuristic and then solve the optimization problem in (65) with an appropriate score for each measurement. This can be formulated as:

1. Select a current pair with some heuristic.
2. Score every measurement connected to this current injection that has not been used previously.
3. Solve (65) for this score.
4. Add selected points to the set of measurements to make.
5. Repeat until enough current injections or potential readings has been selected.

This outline can be combined with the 'spread mass centers' method — the current injection chosen as the current injection used in the measurement furthest from the set of selected measurement so far. The score for each measurement is the distance to the set of selected measurement so far as calculated in section 6.2. The method is initialized by selecting the current injection with the measurement closest to the average mass center.

The outline can also be combined with the 'correlation' method — the current injection chosen as the current injection used in the measurement lowest maximum correlation with the set of selected measurement so far. The score for each measurement is $1 - C$ where C is the maximum correlation with all measurement previously selected as calculated in 6.3.

Both of these methods have a common problem and that is that the score for a measurement is not independent of the other measurements allocated to the board at the same time. This was combated with pre-processing prior to solving (65) which will be discussed more in detail in the next section.

8 Implementation

All of the optimization methods are implemented in matlab. The simulations for a known model of the subsurface, other than that of homogeneous ground, are made with Res2dmod and Res2dinv.

8.1 Electrode layout

The considered electrode layouts are equidistant lines with 64 electrodes and 30 electrodes. The 64 electrode line was spaced with 2.5 meters and the 30 electrode line was space with 5 meters. Every other electrode is used for current

injection and the other half is used for potential measurements. This is useful for several reasons — it makes sure no reciprocal measurements are used so that these may be used for separately in a field measurement, it reduces the total number of measurements making the algorithms less memory and time consuming and it removes the problem of polarization that occurs when using a electrode previously used for a current injection as a potential electrode to soon afterwards.

The layouts were selected for different reasons: the 64 electrode layout is useful for testing the feasibility of the optimization algorithms for larger problems as well as showing the usefulness of the multichannel scheduling. As the multichannel algorithm discussed here is limited to a maximum of 64 electrodes this is the 'worst case scenario' considered in this report. The 30 electrode layout is mostly useful for comparison with the methods discussed in [9], but it is also useful to check the effectiveness of the multichannel optimization for smaller arrays. Both of the arrays will be tested on similar synthetic models of the subsurface..

In the calculations of the sensitivity the ground was assumed to be homogeneous with resistivity $\rho_0 = 1$. The sensitivty used was the 2D-senstivity function. The domain of interest was chosen between $\frac{1}{2}$ electrode distance outside of the electrode layout on either side in the x-direction and from $\frac{1}{8}$ electrode distance to $\frac{e_{num}-1}{4} + \frac{1}{8}$ electrode distances in the z-direction.

8.1.1 Pre-processing

Measurements with high geometric factor are removed from the considered set, due to their poor noise performance as discussed previously. The threshold for geometric factor was set to 5500 m, which is the same as in [9], which is quite a bit lower than the 39396 m threshold in [8] (this article does however use a shorter spacing of 4.75 meters). Both [9] and [8] suggest removing measurements of the γ type due to stability issues in the inversion process so this was also done.

In order to avoid high memory usage pre-processing of the set of all possible measurements can be done. The 'spread mass centers' method seems well suited for pre-processing tasks as it is not that computationally complex and the resulting set has a very similar sensitivity pattern compared to the full set as we will see in later.

8.2 Calculation of sensitivity

The sensitivity, no matter the number of spatial dimensions considered, for an array of 4 electrodes is calculated by simply adding contributions from the 4 different current pole-potential pole pairs. When calculating the sensitivity function for all possible arrays it is therefore possible to calculate the sensitivity of each pair of electrodes first and then recombined these to get the full

sensitivity for each measurement. This avoids calculating the sensitivity contribution of a pole-pole pair of electrodes more than once. The sensitivity in each discretization point is stored in a $m \times n$ where m is the number of considered measurements and n is the number of discretization points. The matrix corresponds to a Jacobian of a function $F : \mathbb{R}^n \to \mathbb{R}^m$ where F_i is the change in the i:th measurement's potential value from a change of the resistivity in the discretization points. This matrix will simply be called J in this paper.

8.3 Res2dinv and Res2dmod

Two softwares, besides Matlab, was used for forward and inverse modelling namely Res2dmod and Res2dinv. In order to get simulated measurements given a synthetic model of the ground Res2dmod was used, the resulting simulated measurements is then read in to Res2dinv, the inversion software. The inversion is done by stipulating a model for the ground, using forward modelling to determine the measurements' responses, compare the responses with the observed response (i.e. the value simulated in res2dmod) and modifiy the model in order to get closer to the observed data. The software uses a modified version of the Marquardt-Levenberg variant of the Gauss-Newton method. The modifications include spatial filters to introduce smooth variations in the model parameters as well as options for using l_1 smoothness constrained optimization. In this thesis l_1 smoothness constrained optimization was used unless specifically stated otherwise, this version of the optimization method will more easily model subsurfaces with sharp edges between sections with different resisitivity. For a better description of the softwares and methods used refer to [6].

8.4 Maximum integral, maximum ratio integral

The set of with the maximum sum over the discretization points can be found by simple sorting:

1. Sum the columns of the J matrix, or use numerical integration.
2. Sort the resulting column vector in descending order.
3. Use the first N measurements as the optimal set.

This easy algorithm will select the individual measurements with the highest integral or sum over the discretization points. The sum of these measurements will have the highest sum possible with N measurements. This works because the sum or integral over the points and the sum over the measurements are interchangeable.

A variant of the above method relies on weighting the discretization points differently - giving some of the points a higher importance than others. One possible weighting function is dividing by the full cumulative sensitivity. The algorithm in this case is:

1. Divide each entry in each row of the J matrix with the corresponding entry in sum of the of the columns of the J matrix (i.e $J_{full} = \sum_i J_i$)
2. Sum the columns of the resulting matrix, or use numerical integration.
3. Sort the resulting column vector in descending order.
4. Use the first N measurements as the optimal set.

This will somewhat deal with the huge differences in sensitivity present in different points of the discretization. None of these two approaches will however spread the measurements in a way that gives smooth sensitivity — in practice it will probably be quite the opposites as a measurement that gives a high integral of the sensitivity function is likely neighboured by a similar measurement that will also get selected.
In the results section these two methods will be referred to as 'Maximum integral' and 'Maximum ratio integral' respectively.

8.5 Correlation

The correlation set begins from a set of measurements where the distance between the current electrodes and between the potential electrodes respectively are smallest possible. This set will be a set of dipoles if the minimum distance between two neighbouring potential electrodes is the same as the minimum distance between two neighbouring current electrodes. Measurements are then iteratively added to the set as described in 6.3. In order to get short execution time the number of added measurements per iteration can be greater than 1. Ideally the number of added measurements could be dynamically selected as a part of the algorithm, in this paper the added measurements per iteration was kept fixed at 16 added measurements per iteration.

This method actively tries to add a measurement that has high sensitivity were the currently selected set does not, i.e. it tries to spread the sensitivity over the subsurface. This method is referred to as the 'correlation' method in the results section.

8.6 Spread mass centers

The algorithm described in 6.2 was directly implemented in matlab. One addition is that for every measurement the symmetric measurement, found by flipping the array around the midpoint of the electrode layout, was also added in each step. This was done in order to get symmetric cumulative sensitivity, but the resulting inversions on simulated data did not improve notably from adding symmetric measurements. Furthermore the x and z locations of the mass centers were normalized to numbers between 0 and 1, this was done in order to give equal weight to spreading in the x and z location as the distances in x is usually much larger than in z. The mass centers were calculated using

the trapezoidal method.

The method is referred to as the 'Spread mass centers' in the result section.

8.7 Multichannel measurements

The goal of the multichannel optimization algorithm is twofold:

1. Find which electrodes to use for current injections.
2. Find which potential measurements to do for the current injection.

We begin by discussing the second item on that list. As presented in the optimization problem (65) there exist a formulation of an optimization problem for selection of which potential measurements to make given that:

1. We know which electrodes are used for the current injection.
2. There exist a score measuring how good each measurement is. The score should also be such that the sum of the scores represents how good a set of measurements is.

Even with these two conditions fulfilled the optimization problem is fairly large — there are a total of 16 variables, with intricate conditions and a non-linear goal function. There is however symmetry in the problem, and that can be abused to find a good solution, if not the best. Further conditions are imposed on the problem in order to make it a bit easier — all electrodes are assumed to be different with a few exceptions. A leaf electrode is allowed to be the same as any other leaf electrode. Link electrode e_2 can be the same as e_8 and link electrode e_5 can be the same as e_{11}.

The used algorithm can be summarized as the following:

1. Select different line electrodes i.e e_1, e_4 , e_7 ,e_{10}.
2. Find the link electrodes with the highest combined score i.e find e_i such that $S(e_{i-1}, e_i) + S(e_{c(i+2)}, e_i)$ is the highest for $i \in \{2, 5, 8, 11\}$. As the link electrodes are assumed to be different from the line electrodes and the conditions in 65 makes it so that for each link electrode we can build a list of candidates that is 6 electrodes long. These would be the 6 electrodes that have the highest combined score as defined above.
3. Cycle through the candidates for each link electrode and find an allocation of all the link electrodes with no contradiction. Stop at the first such allocation. We have now built the 'main loop' of the graph in 4. The value of the link electrodes will determine the value of s_1, s_2, s_3 and s_4 i.e. the switches.
4. Find the highest scoring leaf electrode for each line electrode.

5. Iterate $1-4$ for each combination e_1, e_4 , e_7 ,e_{10} and pick the allocation with the highest cumulative score.

6. Check if there are any measurements allocated that has a score of 0, signifying that the measurement cannot be made either because it has already been selected in a previous current injection, it has too high geometric factor or is a γ-array. These measurements are *not* to be taken and are removed from the allocation (this is the same as removing and edge in the graph 4). Note that it is no problem for the allocations total score that these measurements are removed as their score was 0 during the optimization process as well hence the removal wont affect the optimum.

A lot of small things can add up to make this algorithm much faster without losing much in terms of performance. For starters not all electrodes need to be considered in the allocation — only the ones that are involved in a potential measurement in combination with the selected current pair. Secondly not all combinations of line electrodes need to be examined. Due to the circular symmetry of the switchboard an allocation of

$$e_1 = \hat{e}_1 \tag{66}$$
$$e_4 = \hat{e}_4 \tag{67}$$
$$e_7 = \hat{e}_7 \tag{68}$$
$$e_{10} = \hat{e}_{10} \tag{69}$$
$$\tag{70}$$

and

$$e_1 = \hat{e}_{10} \tag{71}$$
$$e_4 = \hat{e}_1 \tag{72}$$
$$e_7 = \hat{e}_4 \tag{73}$$
$$e_{10} = \hat{e}_7 \tag{74}$$
$$\tag{75}$$

will have the same optimal solution — everything is just rotated. This alone cuts the number of combinations of line electrodes by a factor 4. But the same thing can be said about reversals. The above allocations are also equivalent to:

$$e_1 = \hat{e}_{10} \tag{76}$$
$$e_4 = \hat{e}_7 \tag{77}$$
$$e_7 = \hat{e}_4 \tag{78}$$
$$e_{10} = \hat{e}_1 \tag{79}$$
$$\tag{80}$$

this cuts the number of combinations by an additional factor of 2. Still the number of combinations of line electrodes will be fairly large which will lead

to long execution times. In order to cut down the execution time even more a pre-selection of which electrodes to consider for the line electrodes can be done by finding the n neighbouring line electrode pairs with the highest score when combine with a single link electrode and requiring that the line electrodes are in at least one of these measurements. This is the same as finding the pairs (e_i, e_j) such that:

$$\max_k S(e_i, e_k) + S(e_k, e_j)$$

attains one of the n highest values for all such pairs. A value of $n = 8$ was used.

Now that a way of selecting a set of potential measurements for a given current pair has been found the next step is to find a way of selecting which current injections to make. For this we will use the following outline:

1. Select an initial set of current injections and potential measurement allocations and add these to the measurement set $\hat{I}$.
2. Score every measurement not in $\hat{I}$ with S_i.
3. Find the top scorer, denote this measurement $\hat{m}$. The current injection used in $\hat{m}$ will be used for this allocation.
4. Build a set of considered measurements by taking all measurements using the same current injection as $\hat{m}$.
5. Score every measurement in the considered set with $\hat{S}_i = S_i$.
6. Solve (65) for the score $\hat{S}_i$. Add these measurements to the set $\hat{I}$.
7. Iterate 2-6 until enough measurements have been chosen.

The method as presented above has two problems:

1. The selected measurements for a given current injection might be similar as the score is only dependent of $\hat{I}$ and of each individual measurement. The score of a given allocation will *not* be the same as the sum of the scores of every measurement in the allocation. The reason is that the measurements in the allocation might, and probably will, have similar sensitivity patterns and thus a lot of duplicate information. This means that the assumption that the score of an allocation is the sum of the scores of every measurement is false when solving (65).
2. The method might not make full use of the multichannel capabilities of the switchboard as it can prioritize very small gains in the score of the select allocation over adding one more slightly lower scoring measurement.

The problems were solved in the following way:

1. A pre-selection of which measurements to consider for a given current injection was used. The pre-selection was made by using either the 'spread mass centers' method or the 'correlation' method for the set of measurements connected to current injection. This should remove measurements that are very similar.

2. The score for a given measurement was changed to $\hat{S}_i = S_i + \frac{\bar{S}}{2}$ where $\bar{S}$ denotes the average score of the considered measurements. This ensures that every measurement has a minimum score — which means that just making more measurements for a current injection is a bit better compared to not using one of the channels on the switchboard.

And the full algorithm can be described as:

1. Select an initial set of current injections and potential measurement allocations and add these to the measurement set $\hat{I}$.

2. Score every measurement not in $\hat{I}$ with S_i.

3. find the top scorer, denote this measurement $\hat{m}$.

4. Use the current injection used in $\hat{m}$.

5. Build a set of considered measurements by taking all measurements using the same current injection as $\hat{m}$ and using either the 'spread mass centers' method or 'correlation' method with $\hat{m}$ as the initial set. The set considered measurements should have size N_{pre} or lower, a pre-fixed parameter.

6. Score every measurement in the considered set with $\hat{S}_i = S_i + \frac{\bar{S}}{2}$ where S_i is score of the i:th measurements.

7. Solve (65) for the score. Add these measurements to the set.

8. Iterate 3-7 until enough measurements have been chosen.

This outline can be combined with a scoring resembling that of the 'correlation' method as well as one resembling the 'spread mass center' method.

8.8 Correlation multichannel method

The previously discussed outline is combined with a scoring:

$$S_i = 1 - \max_{j \in \hat{I}} C_2(|J_i|, |J_j|) \tag{81}$$

where C_2 is defined in equation (60). The value of C_2 is approximated with the Pearson correlation as found in equation (64). A higher score is better, meaning that we want the maximum correlation with the so far selected set to be as low as possible — this is the same idea as in the 'Correlation' method. The added 1 is there to make sure that the score is non-negative.

The considered set was built with the 'Correlation' method, and N_{pre} was selected as 128. The initial set is built by selecting the current injections where the distance between the electrodes is as small as possible and solve problem (65) with each measurement scored as:

$$S_i = \int_A \frac{|J_i(\mathbf{x})|}{\sum_{j \in I_{all}} |J_j(\mathbf{x})|} \, \mathrm{d}\mathbf{x} \tag{82}$$

i.e the integral of the absolute sensitivity divided by the cumulative absolute sensitivity of the full set.

8.9 Spread mass centers multichannel method

The method is meant to be a multichannel variant of the 'spread mass centers' method. The scoring used is

$$S_i = \min_{j \in \hat{I}} |\mathbf{m}_i - \mathbf{m}_j| \tag{83}$$

where $\mathbf{m}_i$ denotes the mass center of the i:th measurement. This means that the score prioritize measurements with a high minimum distance to the set which is the same idea used in the 'spread mass centers' method.

The considered set was built with the 'spread mass centers' method, and N_{pre} was selected as 128. The initial set is built by selecting the current injection closest to the mass center of the cumulative absolute sensitivity and solving problem (65) with the score being the distance to this mass center.

9 Results

9.1 Sensitivity patterns

We will now look at the absolute cumulative sensitivty patterns for the discussed methods aswell as the ratio of these sensitivity patterns and the full set of measurements sennsitivity pattern.

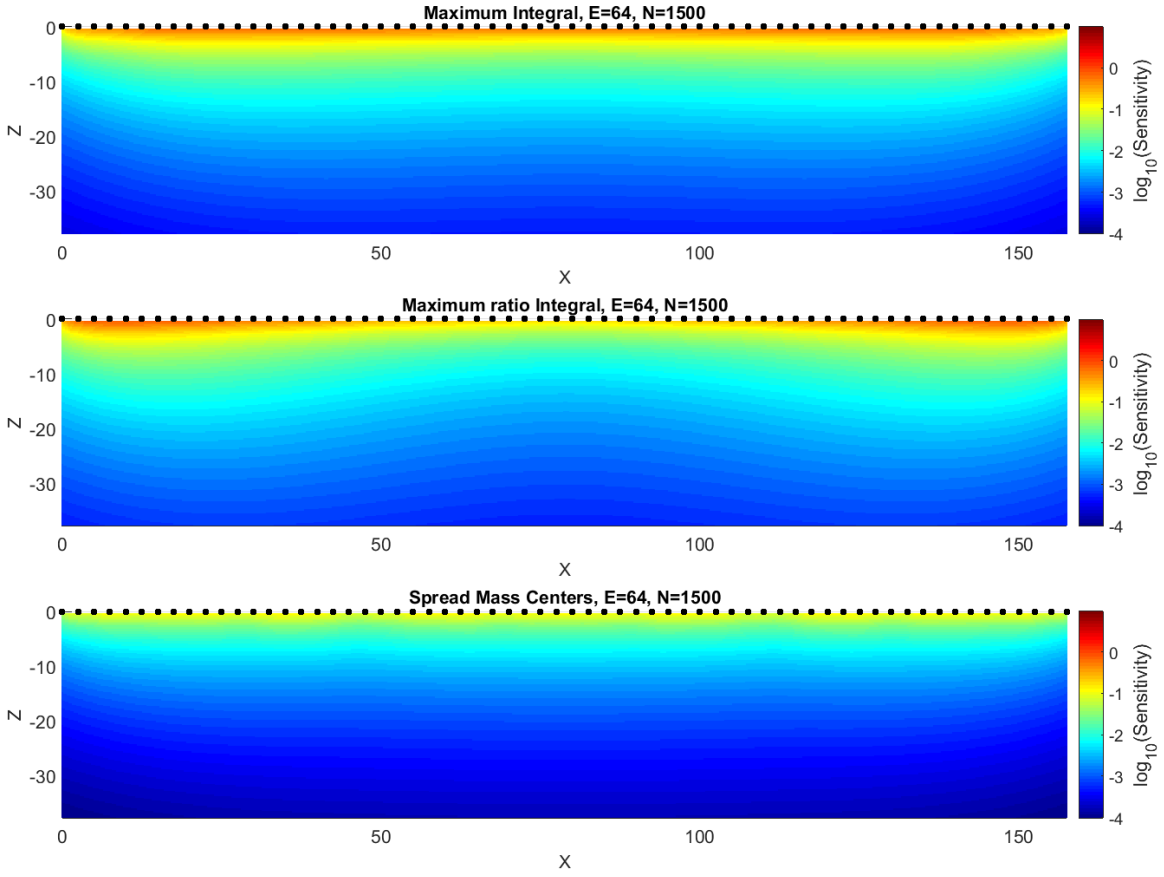

Figure 5: The 'Maximum Integral', 'Maximum ratio Integral' and 'Spread Mass centers' methods' optimal sets' cumulative absolute sensitivity for a 64 electrode layout. The number of measurements in the optimized set is approximately 1500.

In figure 5 we see the cumulative sensitivty for the 'Maximum integral', 'Maximum ratio Integral' and the 'spread mass centers'-methods. Note how both of the integral methods seem to have higher sensitivity overall and in particular in the area nearest the surface. We can also see that the 'maximum ratio integral' method seem to prioritize high sensitivity to the side of the electrode layout.

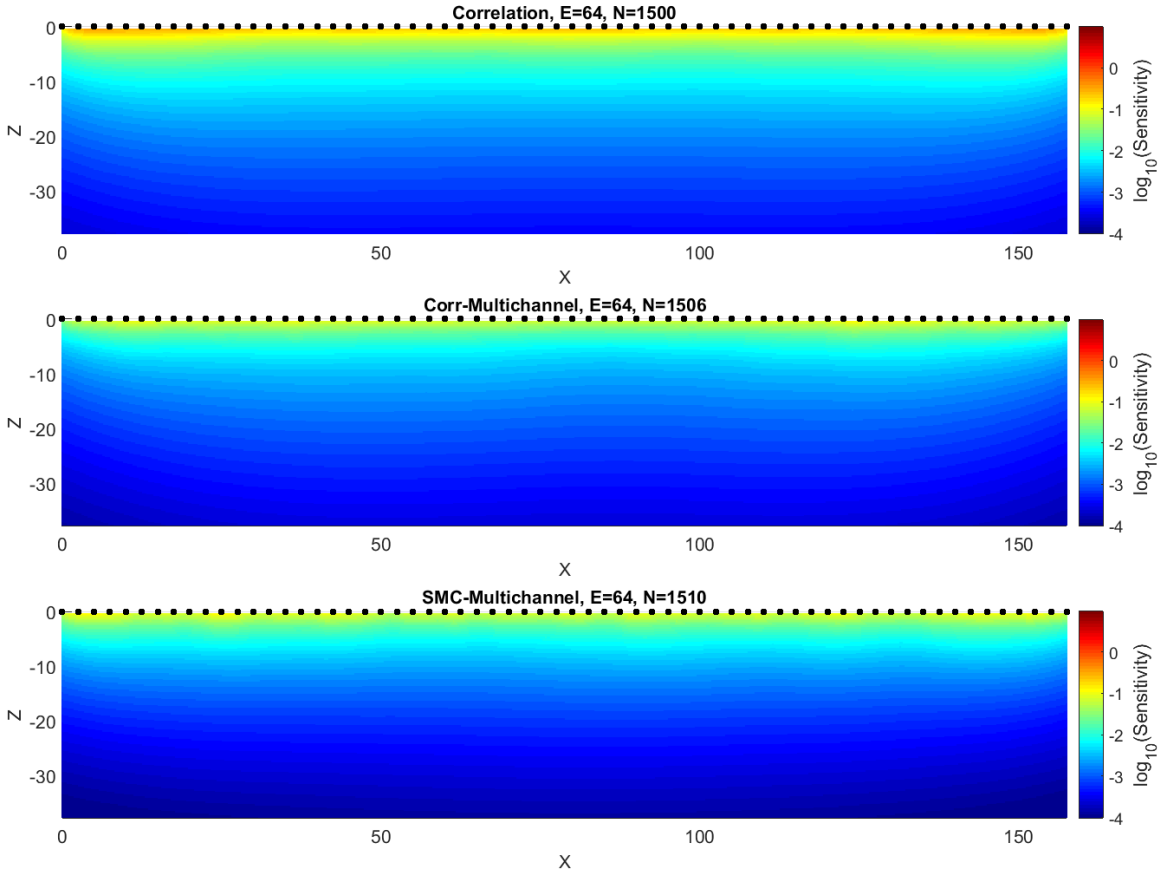

Figure 6: The 'Correlation', Corr-Multichannel and 'SMC-Multichannel' methods' optimal sets' cumulative absolute sensitivity for a 64 electrode layout. The number of measurements in the optimized set is approximately 1500. Both of the multichannel methods have low cumulative absolute sensitivity. Compared to the other methods.

In figure 6 we see the cumulative sensitivty for the 'Correlation', Corr-Multichannel and 'SMC-Multichannel' methods. The 'SMC-multichannel' method have a clearly lower sensitivity everywhere. The 'Correlation' and 'Mulitchannel' method seem to both prioritize measurements far to the side.

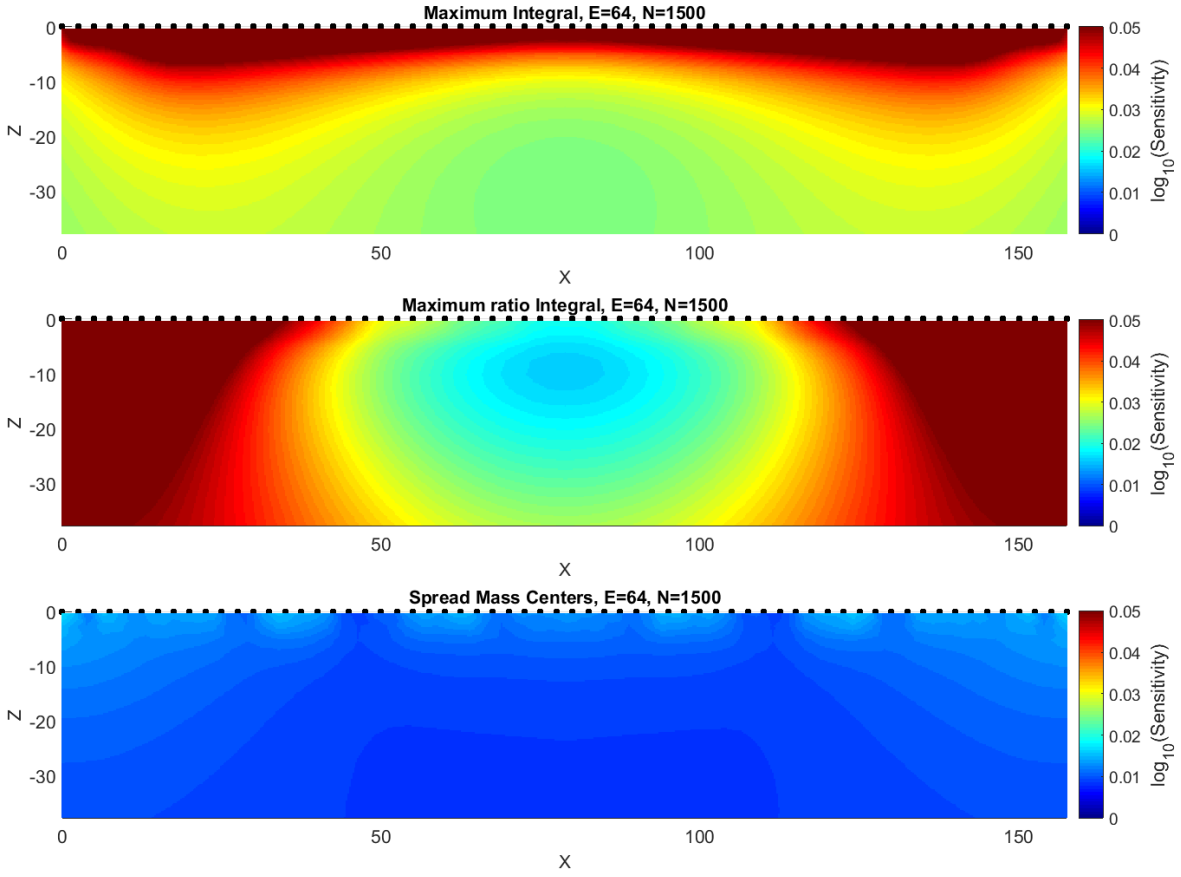

Figure 7: The ratio between the 'Maximum Integral', 'Maximum ratio Integral' and 'Spread Mass centers' methods' optimal sets' cumulative absolute sensitivity and the comprehensive set's cumulative absolute sensitivity for a 64 electrode layout. The number of measurements in the optimized set is approximately 1500.

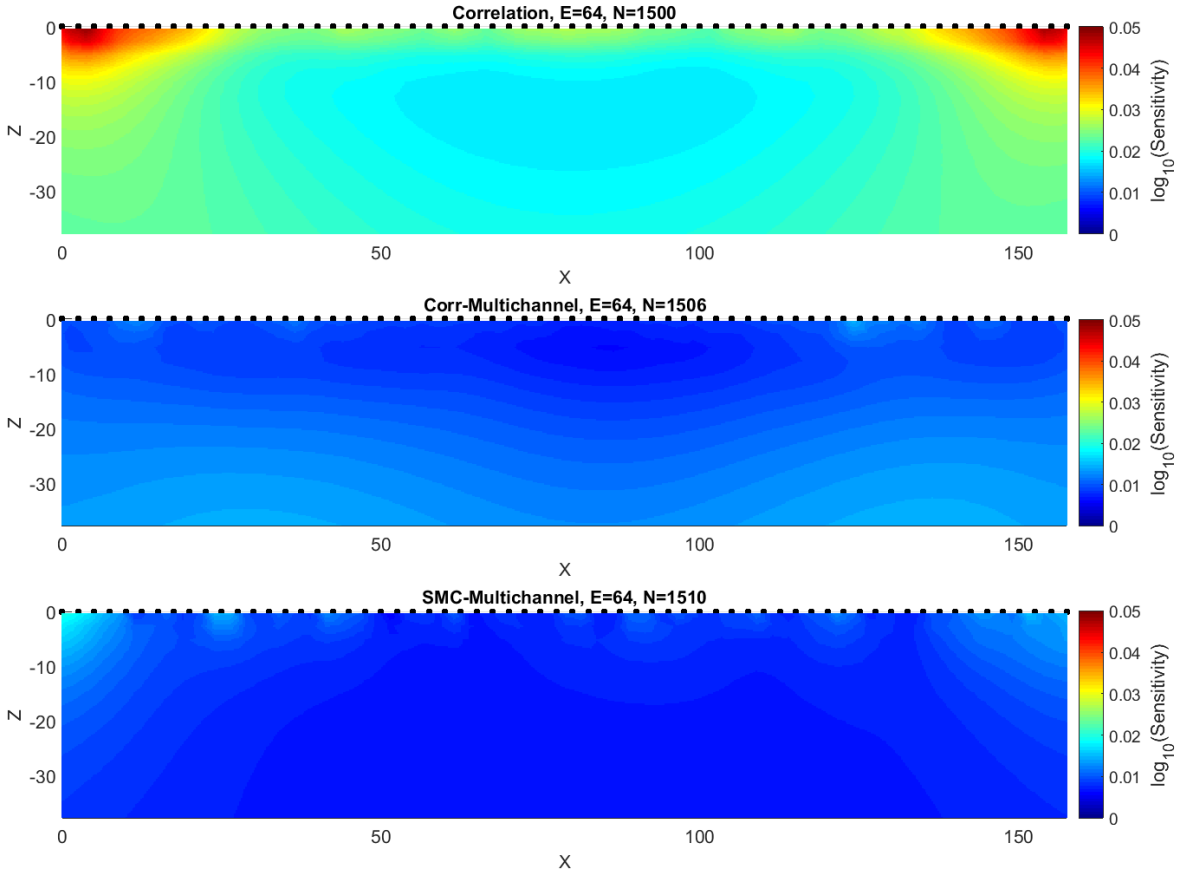

Figure 8: The ratio between the 'Correlation', Corr-Multichannel and 'SMC-Multichannel' methods' optimal sets' cumulative absolute sensitivity and the comprehensive set's cumulative absolute sensitivity for a 64 electrode layout. The number of measurements in the optimized set is approximately 1500.

In the relative sensitivity figures we can clearly see that the integral methods and to some extent the 'correlation' method seem to but a lot of weight to the sides compared to the comprehensive set. We can also note that the methods based on the spread mass center method seem to have lower general sensitivity but it is more evenly spread.

9.2 Simulations

Apparent resistivity values were simulated with 'Res2Dmod' for the following synthetic ground:

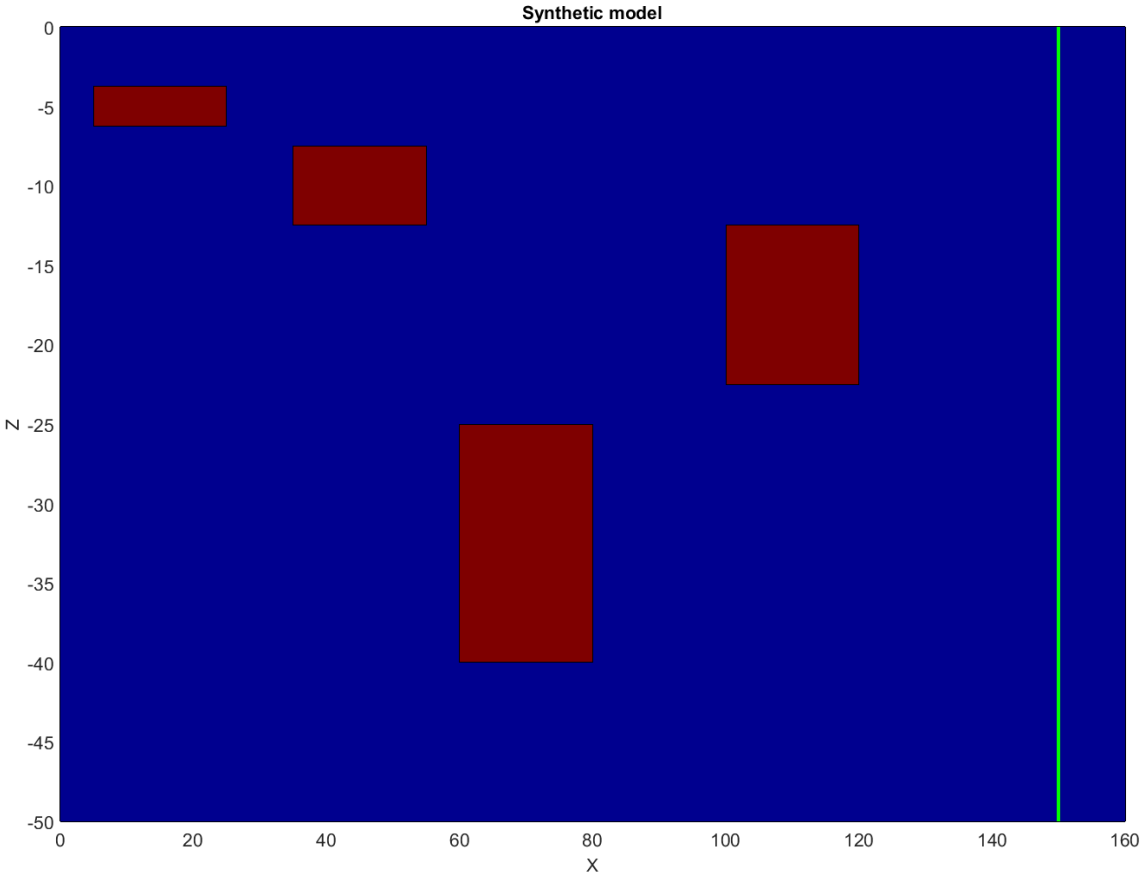

Figure 9: The synthetic model used for simulations. The red prisms have a resistivity of $100\Omega \cdot m$ while the background has $10\Omega \cdot m$ The green line shows where the 30-electrode layout ends. The 64-electrode layout goes all the way to $X = 160$.

9.2.1 Results for a 64 electrode array

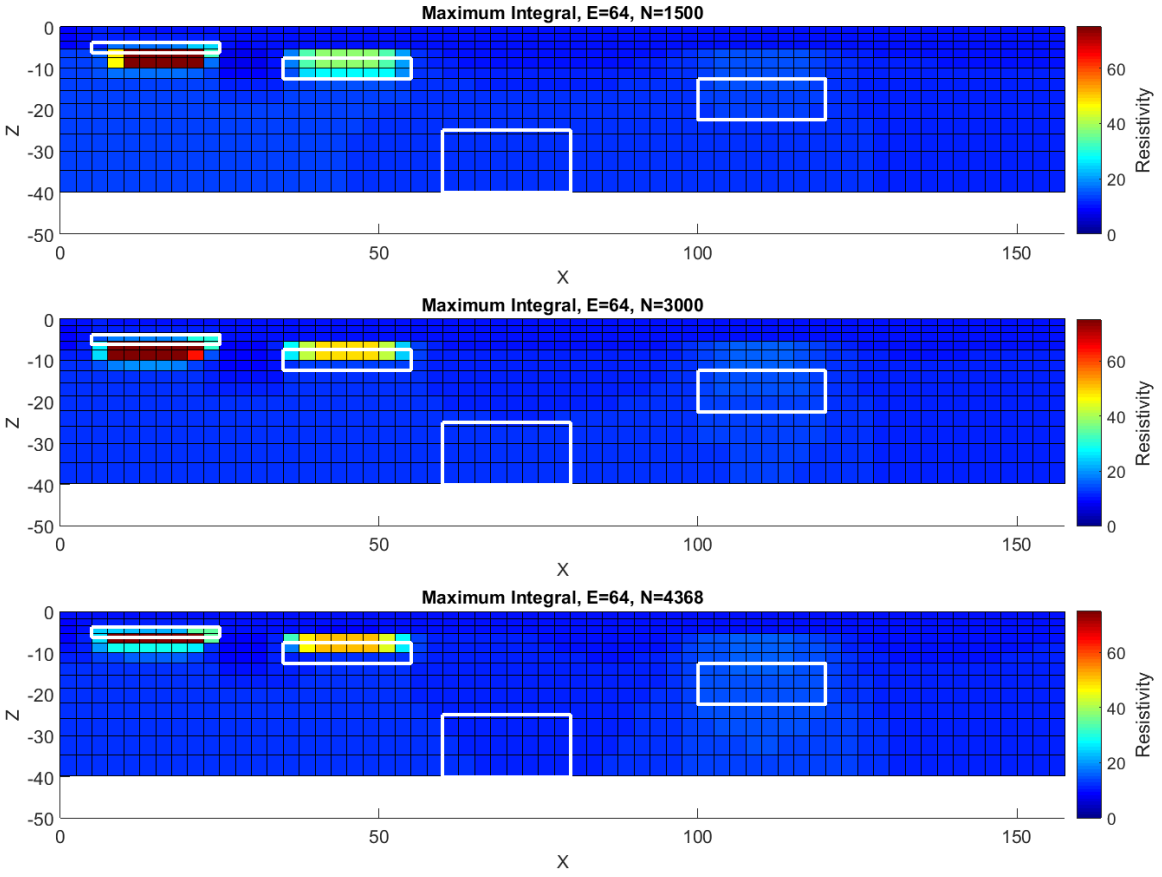

Figure 10: The modelblocks used for inverting simulated data and their inverted resisitivity value and their inverted resisitivity value. The set of measurements is generated by the 'Maximum integral' method. The total number of electrodes in the array is 64 spaced with 2.5 meters. The white stripe at the bottom is an area where the inversion software deemed that there was too little information in the measurements to model.

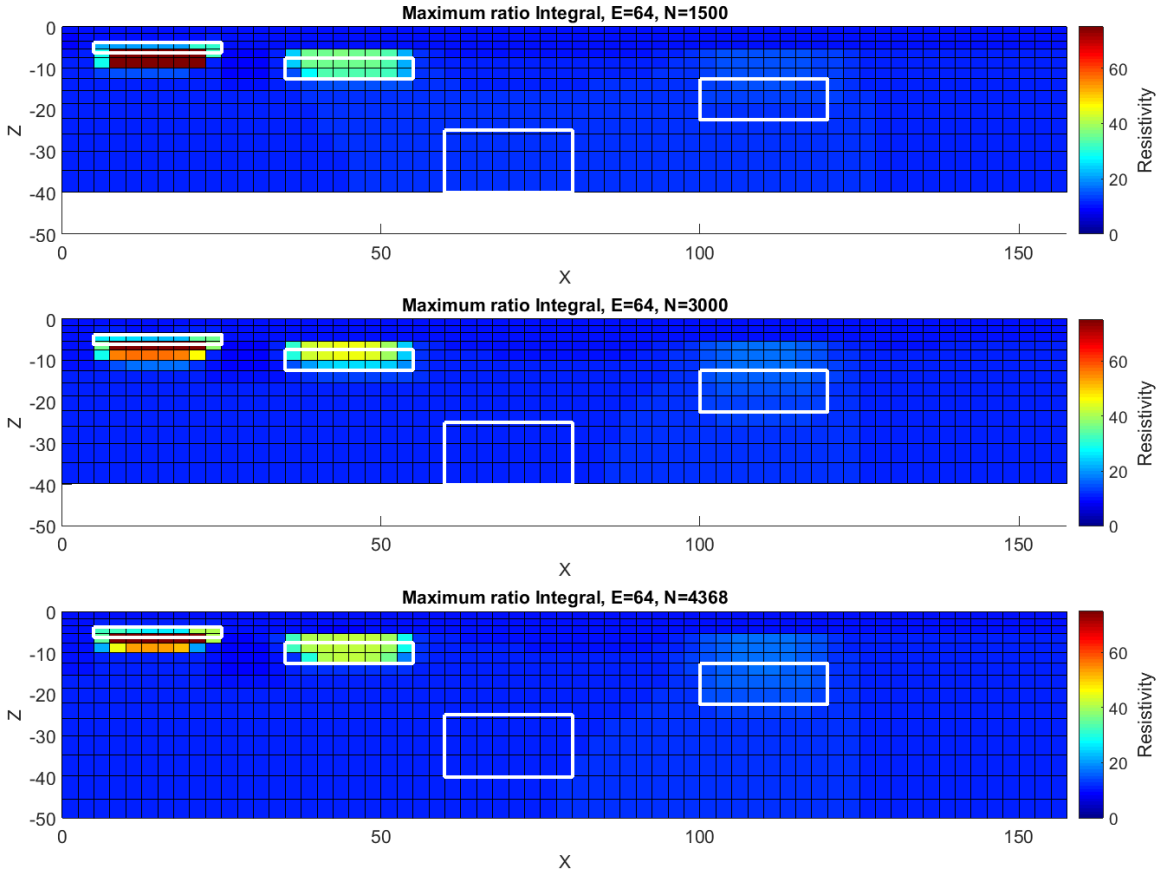

Figure 11: The modelblocks used for inverting simulated data and their inverted resisitivity value and their inverted resisitivity value. The set of measurements is generated by 'Maximum ratio integral' method. The total number of electrodes in the array is 64 spaced with 2.5 meters. The white stripe at the bottom is an area where the inversion software deemed that there was too little information in the measurements to model.

In both figure 10 and 11 we can see a clear failure of resolving the far right and deepest prism. This is probably due to a heavy overlap within the select measurements for these two methods — there are comparatively many measurements that measure the same, or close to the same, area of the subsurface. These methods also seem to prioritize methods with high sensitivity close to the surface. This is probably due to measurements with high total sensitivity are usually mostly sensitive to the top layer of the subsurface and that most of the

sensitivity to changes in the deeper parts of the subsurface comes from small contribution from a large number of measurements while closer to the surface most of the sensitivity comes from a few measurements with large contributions. All in all these methods are not recommend for use other than benchmarking if they are not modified to take more spatial information into account.

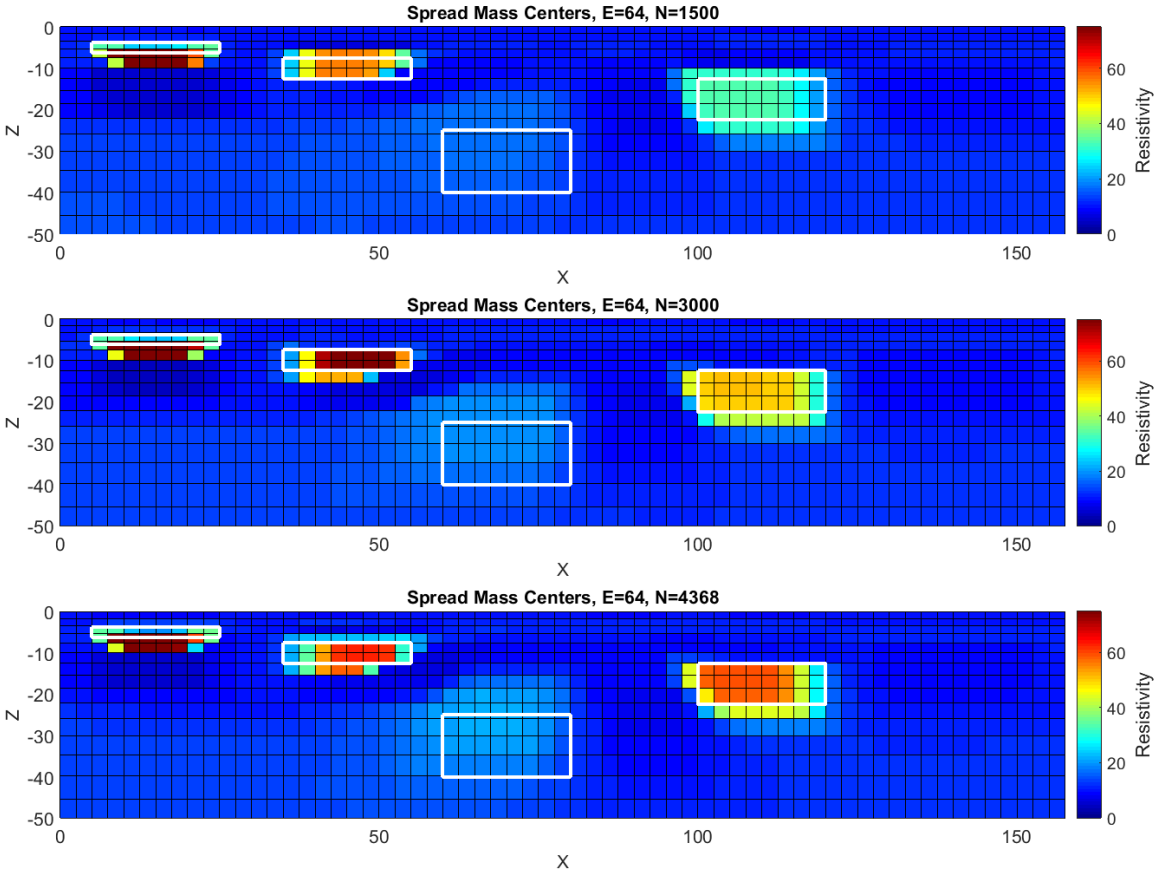

Figure 12: The modelblocks used for inverting simulated data and their inverted resisitivity value and their inverted resisitivity value. The set of measurements is generated with the 'Spread mass centers' method. The total number of electrodes in the array is 64 spaced with 2.5 meters.

In figure 12 we can see the quality of the inversion getting much better as the number of measurements increases — in fact this is probably the method which seems to improve the most by adding more measurements. We can see

the imoprovement on the far right prism as well as the deepest prism: the far right prism gets a stronger and stronger response with a greater contrast to the background resisitivity distribution and the deepest block, while not clearly resolved, also get a clearer response.

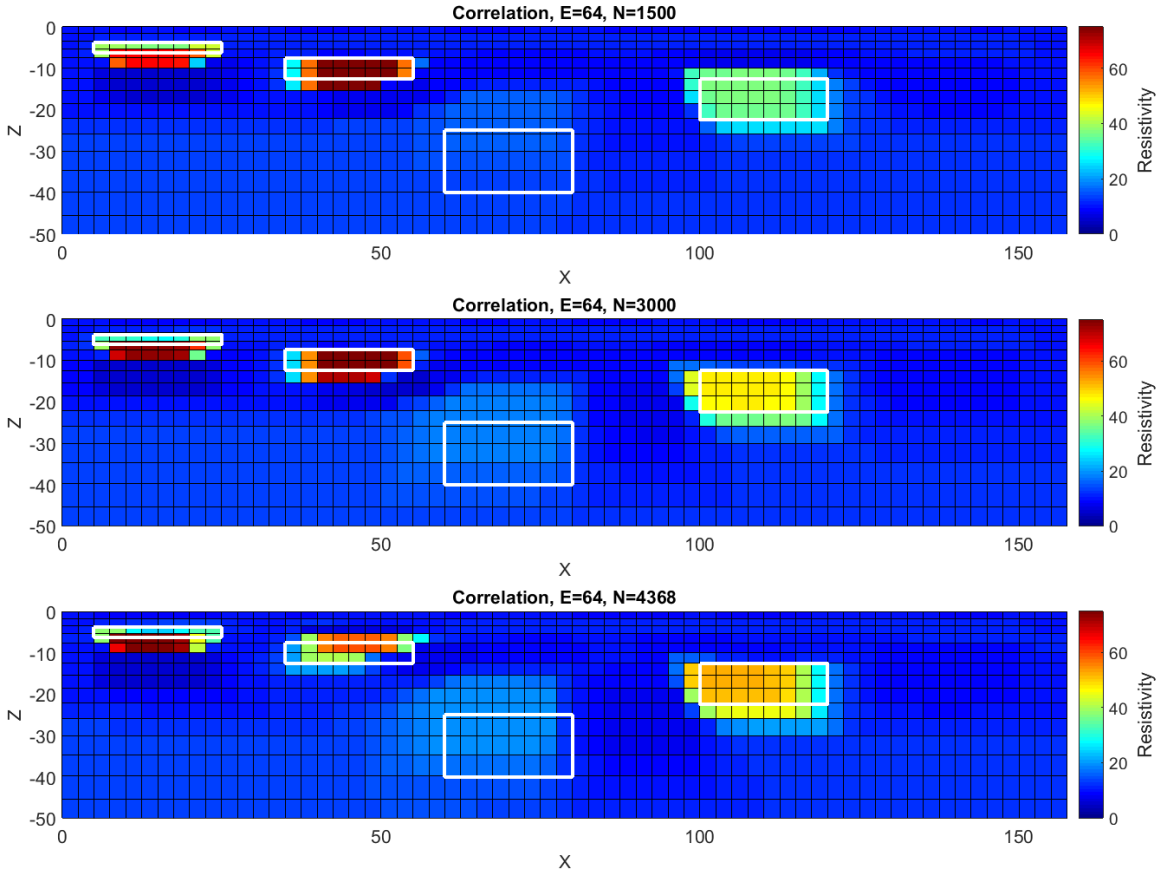

Figure 13: The modelblocks used for inverting simulated data and their inverted resisitivity value. The set of measurements is generated with the 'Correlation' method. The total number of electrodes in the array is 64 spaced with 2.5 meters.

In figure 13 we can see the quality of the inversion in the rightmost block getting better as the number of measurements increases, but not as good as the improvements for the 'spread mass centers' method. We can see improvement in the resolution of the deepest prism aswell although it is still not clearly resolved.

The method does however, somewhat weirdly, resolve the second block from the left worse with the largest set.

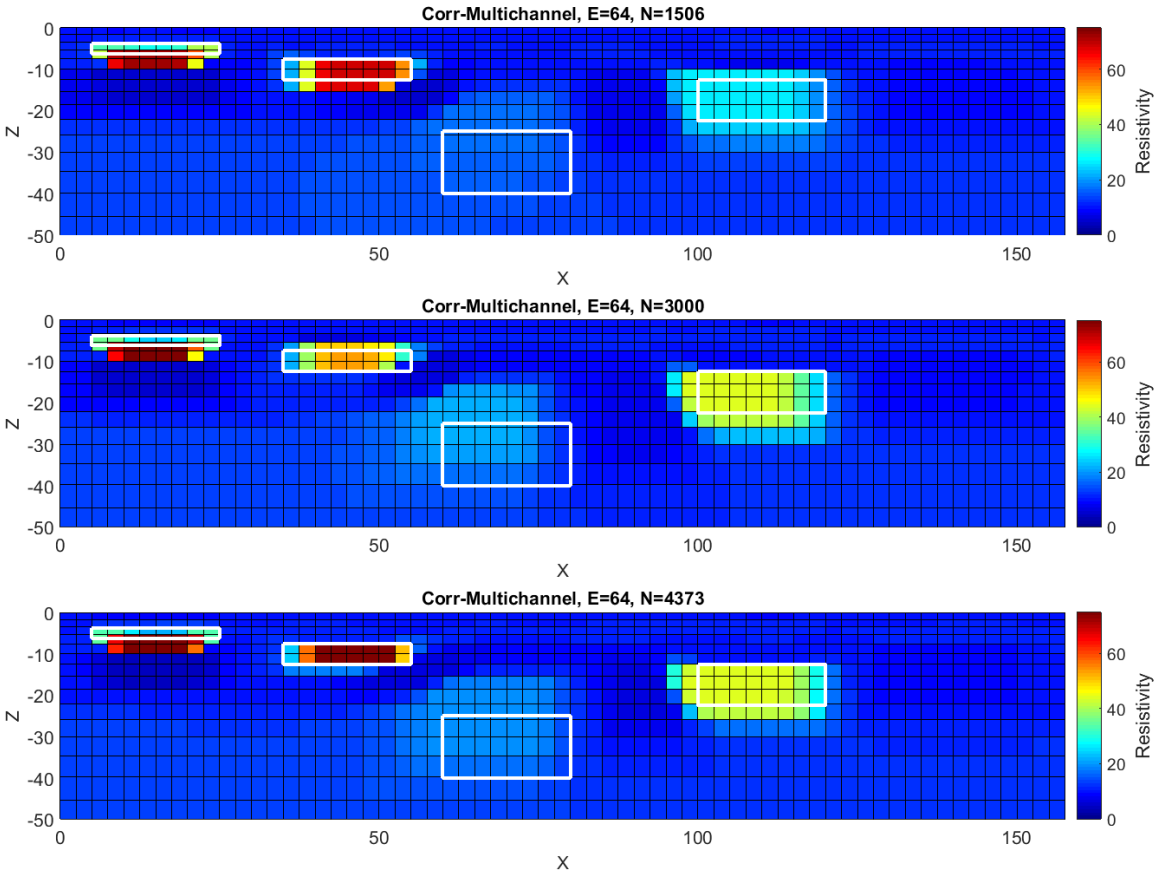

Figure 14: The modelblocks used for inverting simulated data and their inverted resisitivity value. The set of measurements is generated with the Corr-Multichannel method. The total number of electrodes in the array is 64 spaced with 2.5 meters.

In figure 14 clear improvement is seen when the size of the set increases. While this method is partially based on the 'correlation' method the added constraint of using the switchboard's capacity to a large extent seems to not hinder it much for large measurement sets. The smallest set does however lag behind its 'correlation' method counterpart, particularly for the rightmost block.

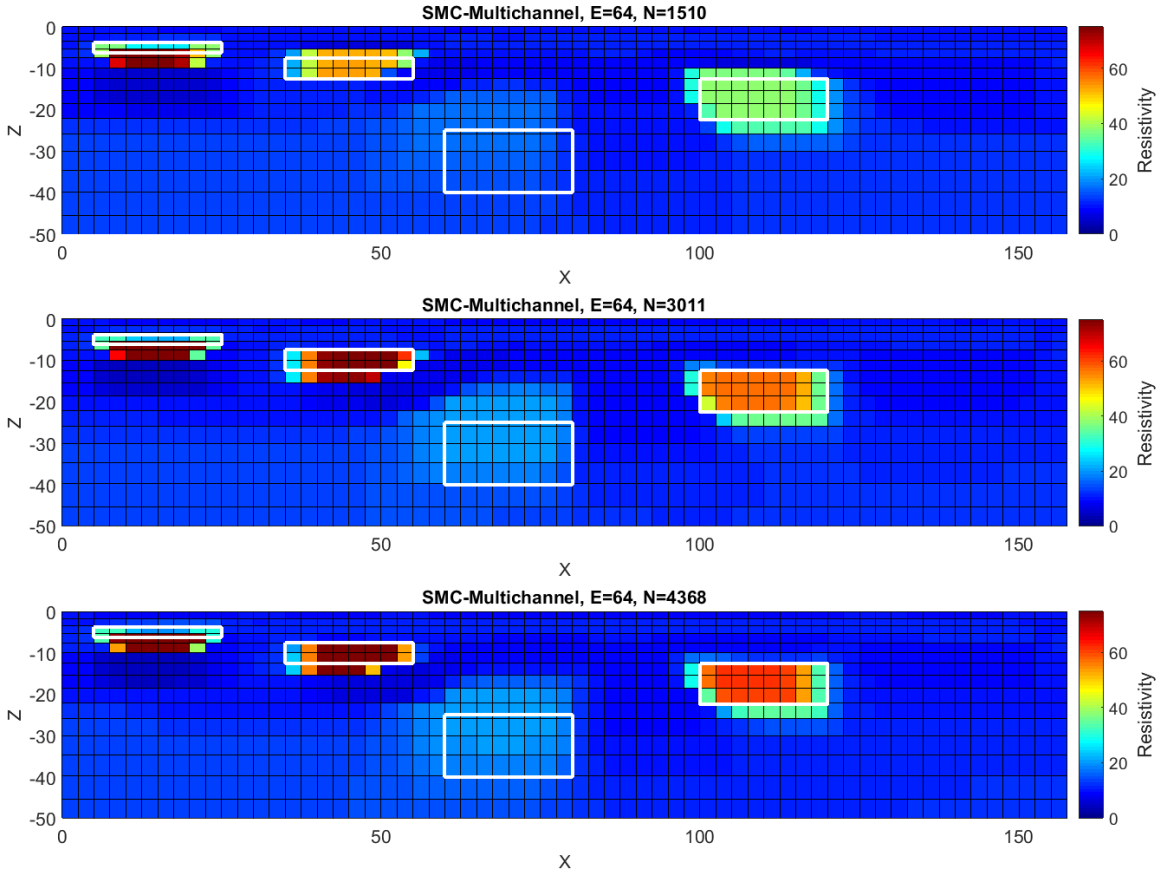

Figure 15: The modelblocks used for inverting simulated data and their inverted resisitivity value. The set of measurements is generated with the 'Spread Mass Centers Multichannel' method. The total number of electrodes in the array is 64 spaced with 2.5 meters.

In figure 15 a clear improvement can be seen when increasing the number of measurements. The method, if working correctly, should try to spread the mass centers of the measurements in a similar way as the 'Spread mass centers' method. This should ensure measurements that are relatively independent. The added constraints of using the switchboards capacity to a large extent does not seem to hinder the method in any obvious way and the results show clear improvement when the measuring set is made larger.

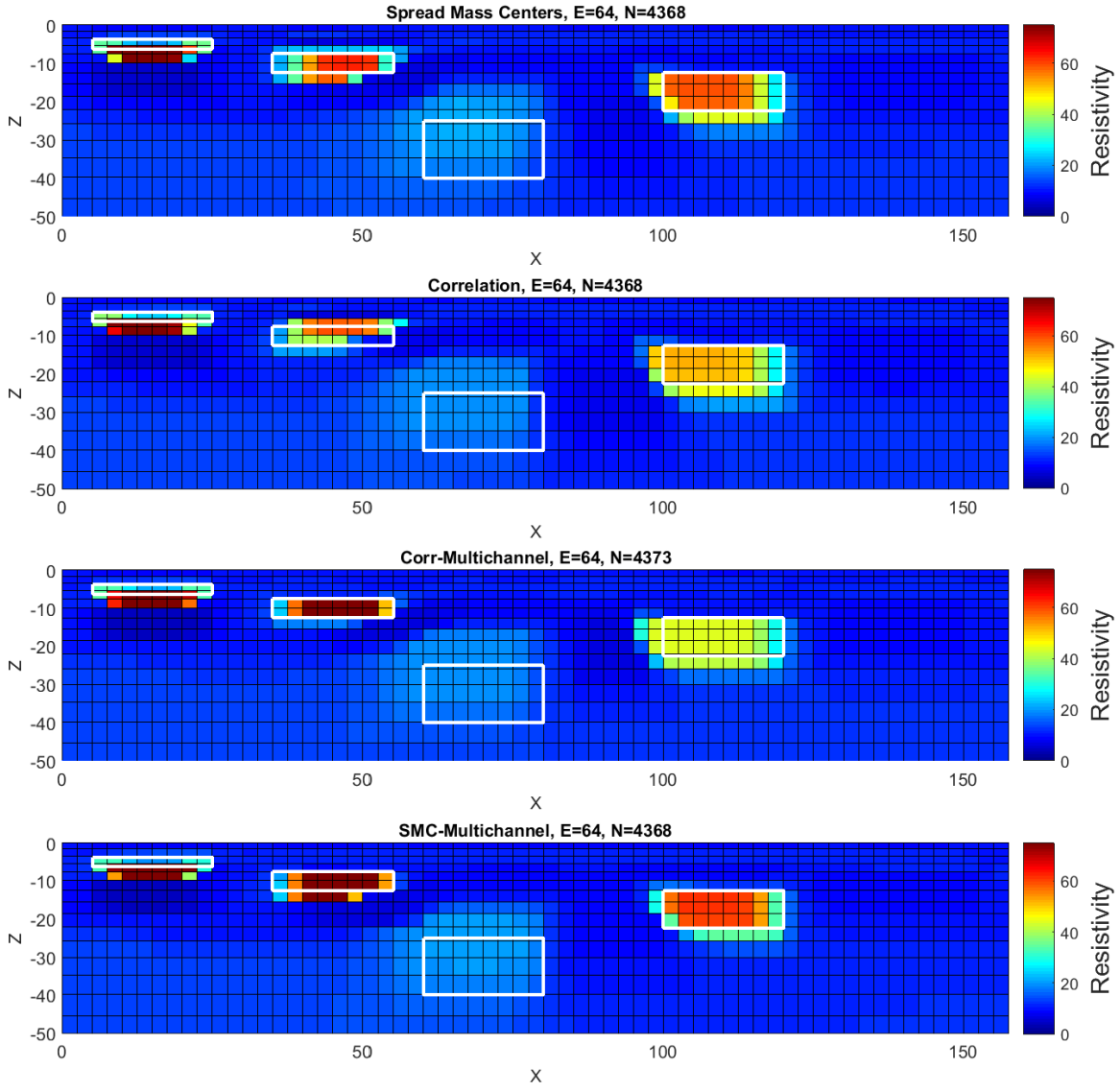

Figure 16: Different methods side by side for approximately 4368 measurements.

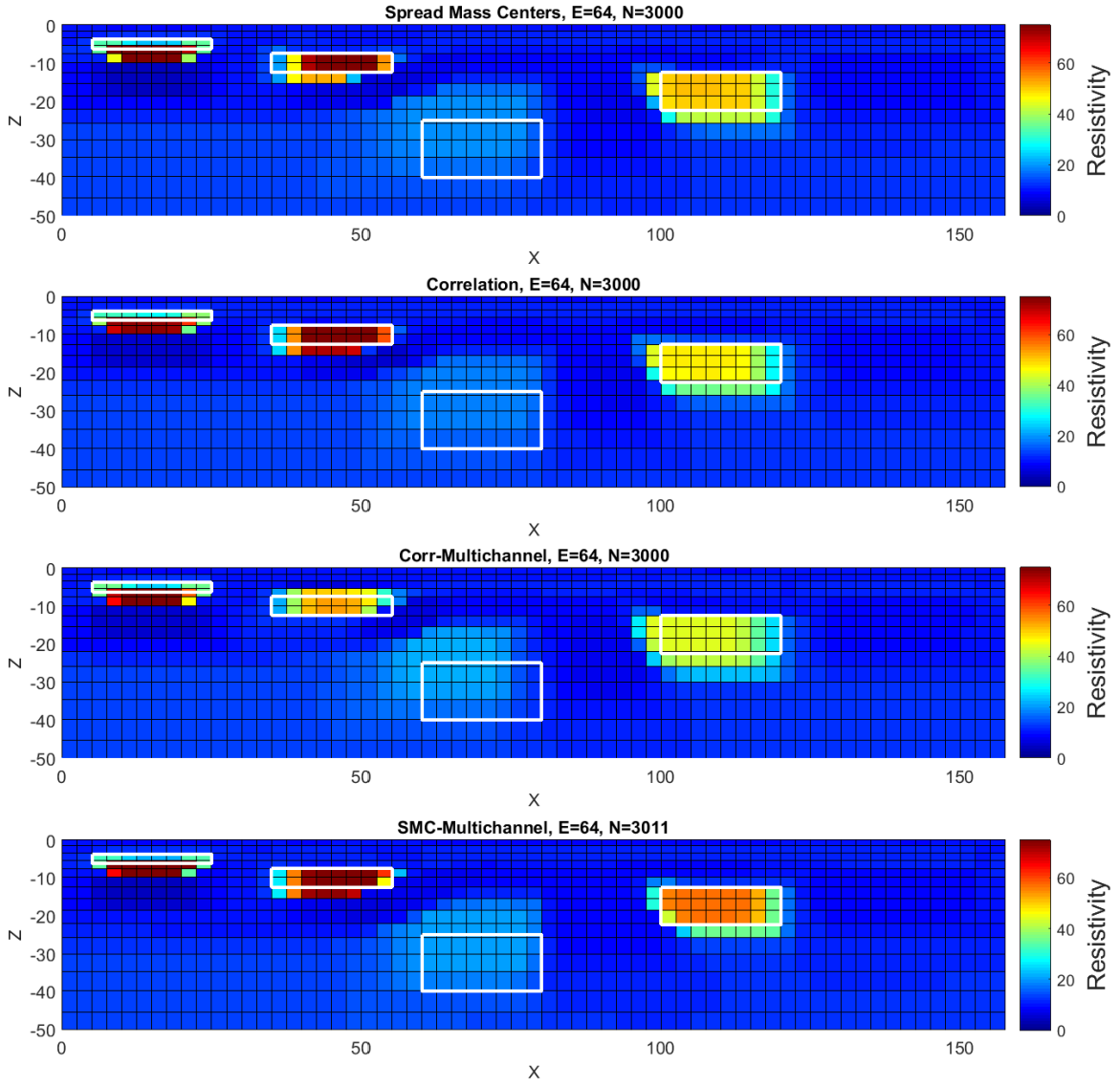

Figure 17: Different methods side by side for approximately 3000 measurements.

In figure 17 we see the different methods compared for approximatley 3000 measurements. The 'Corr-Multichannel' method has a worse estimate of the

restistivity in the second prism from the left than all the other methods. It is clear that for this synthetic model and this many measurements the protocols based on the spread mass centers approach outperforms the methods based on correlation and the same conclusion can be drawn from figure 16.

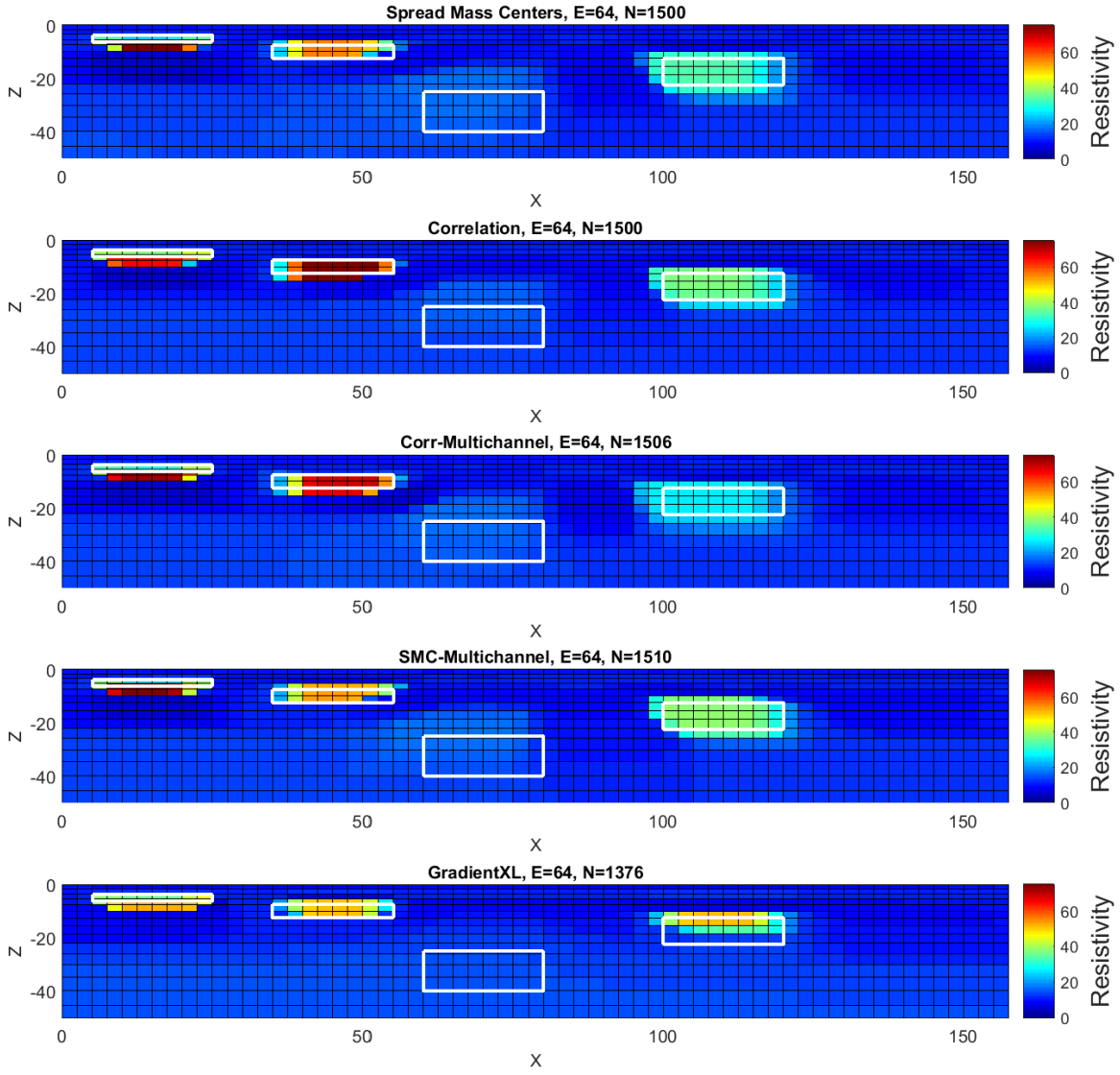

Figure 18: Different methods side by side for approximately 1500 measurements.

In figure 18 we see the different methods compared for approximatley 1500 measurements. The four methods in this plot that has been developed in this

paper show similar results to one another — the two left prisms are relatively well resolved in all cases, the far right prism has a bit lower resisitivity and the deepest block is only present as a small indication if at all represented. The 'Corr-Multichannel' method has the worst approximation of the resistivity of the rightmost block, but all the other perform very similarly. In this plot there is also a multichannel standard script supplied with the instrument called 'GradientXL'. The gradient protocol stands out from the rest of the results by having a more concentrated far right block — underestimating the size of the block where most of the other methods overestimate it. The gradient protocol also has the lowest resistivity in the first prism from the left.

9.2.2 Results for a 30 electrode array

Below the results for a 30 electrode layout is shown. The main point of this section is twofold:

1. Show of the proficiency with which the multichannel optimized protocols schedule measurements i.e. how many measurements is on average taken for every current injection. The average measurements per current injection is expected to decrease compared to the 64 electrode case due to the much smaller number of possible measurements.

2. The 30 electrode layout and the model of the sudsurface is chosen to be similar to the situation in [9]. The results presented here should be comparable to the results in this article, although the inversion parameters and the subsurface model is not exactly the same — it is important to keep this in mind when comparing. For a much more accurate comparison the methods would have to be compared side by side for the same inversion parameters and model.

With this in mind we will only compare the multichannel protocols, the 'correlation' and the 'spread mass centers' method, for the rest of the methods the results for 64-electrodes is deemed enough for drawing the relevant conclusions about their performance. The following two images showcase the performance of the 'correlation' method and the 'spread mass centers' method when using all electrodes as for either current injection and potential readings. The result are very similar — the only big difference is a more concentrated prism to the far right for the 'correlation' method and the highest number of measurements. These figures should be somewhat comparable to the results in [9], as it is a similar model of the ground with the same electrode layout. The exact synthetic model was not published as a part of this article nor was the inversion parameters used for solving the tomographic problem — this combination implicates that one should be careful when drawing conclusions when comparing the results.

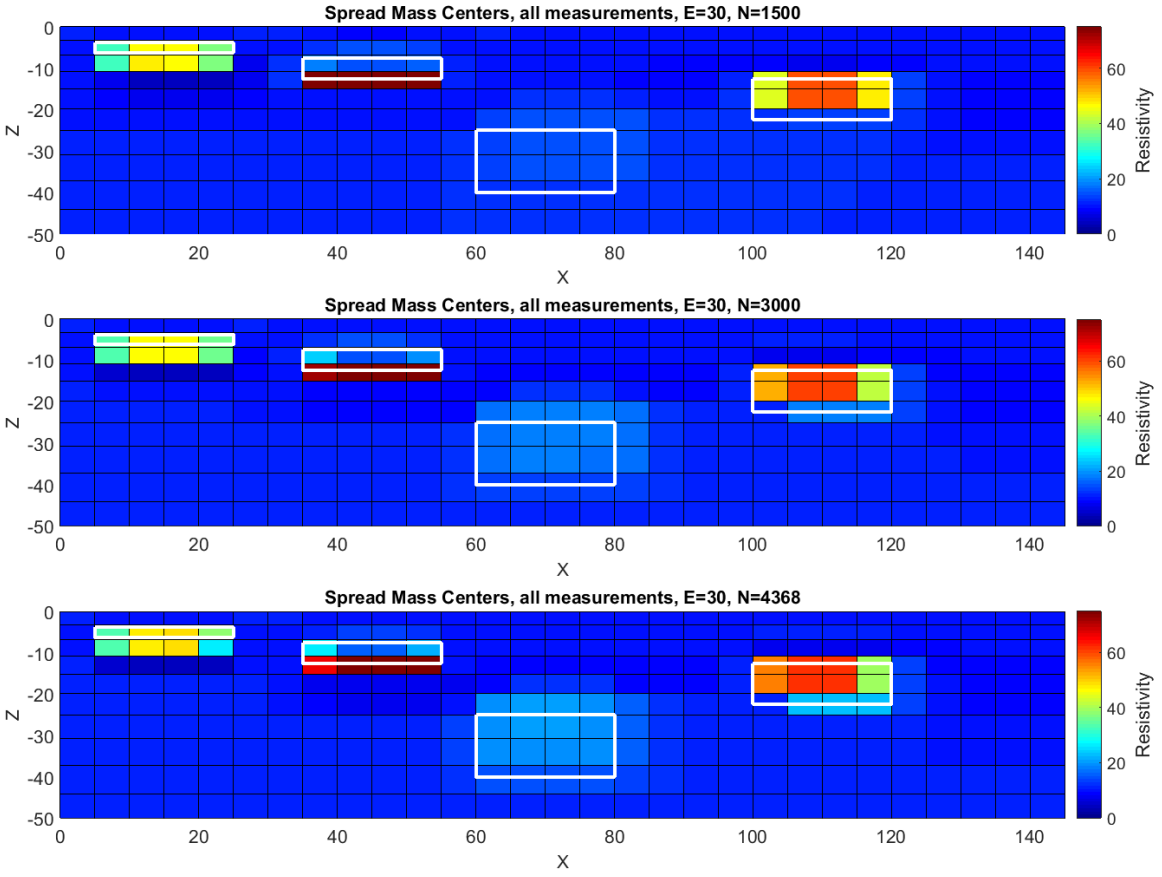

Figure 19: The modelblocks used for inverting simulated data and their inverted resistivity value. The set of measurements is generated with the 'Spread mass centers' method. The total number of electrodes in the array is 30 spaced with 5 meters, in this case all of the electrodes could be used for either current injection or potential readings leading to 51373 possible measurements after removing measurements with too high geometric factor.

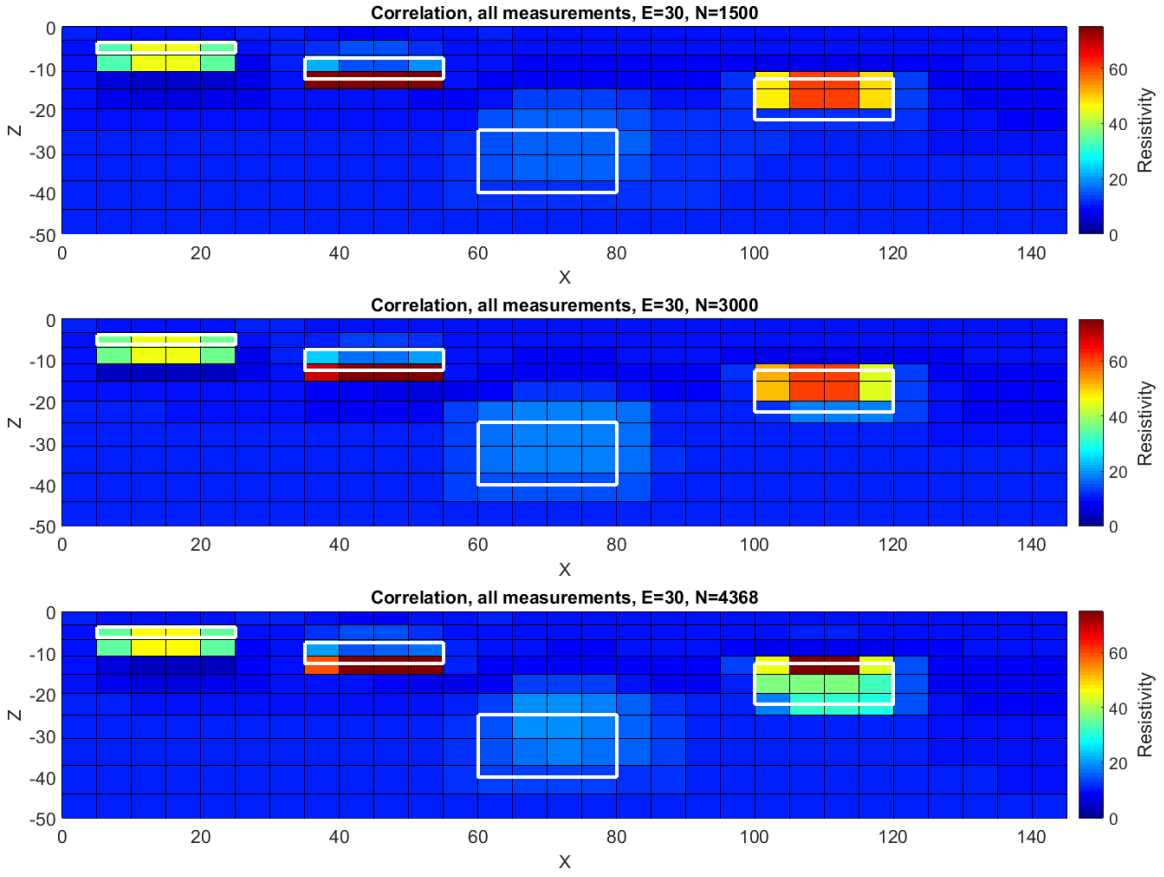

Figure 20: The modelblocks used for inverting simulated data and their inverted resistivity value. The set of measurements is generated with the 'Correlation' method. The total number of electrodes in the array is 30 spaced with 5 meters, in this case all of the electrodes could be used for either current injection or potential readings leading to 51373 possible measurements after removing measurements with too high geometric factor.

The following two figures are meant to showcase the performance of the multichannel protocols when used for a smaller set of electrodes than 64. In terms of consistency the 'spread mass center multichannel' protocols inverted resitivity does not change much as the number of measurements increases. This is probably due to a very small comprehensive set — only 6585 possible measurements remain for the multichannel methods to choose from after removal of γ arrays and measurements with too high geometric factor. This means that

the algorithms will select a large percentage of the comprehensive set compared to the case when a 64 electrode layout was used.

The 'corr-multichannel' method has clearly worse results for $N \approx 1500$, as seen in the second prism from the left. The prism to the far right is also more concentrated for $N \approx 3000$.

One can also note that the 'spread mass center' and 'spread mass center multichannel' results are close to identical even tough the single channel method has access to more possible measurements. This indicates both that the loss in resolution from using every other electrode as a current injector and rest as potential readers does not lower the resulting protocols resolution too much. We can also conclude that the multichannel scheduling seems to work— we get the same basically inverted resistivity with 'spread mass center' and 'spread mass centers multichannel'. The same can not be said about the methods based on correlation — this can be seen in the figures presented in this subsection as well as figure 16 - 18.

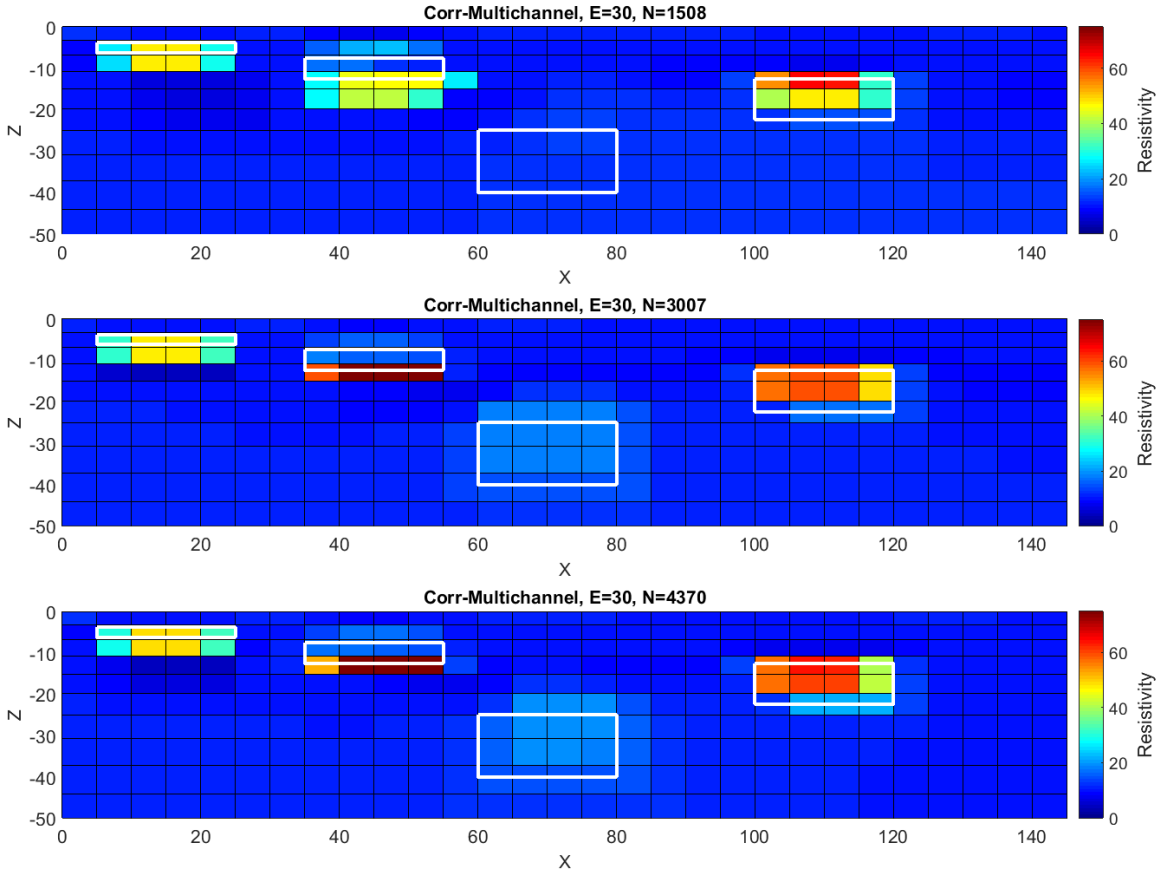

Figure 21: The modelblocks used for inverting simulated data and their inverted resisitivity value. The set of measurements is generated with the 'Corr-Multichannel' method. The total number of electrodes in the array is 30 spaced with 5 meters. Only every other electrode could be used for current injection and the rest could be used for potential readings leading to a total of 6585 possible measurements to choose from.

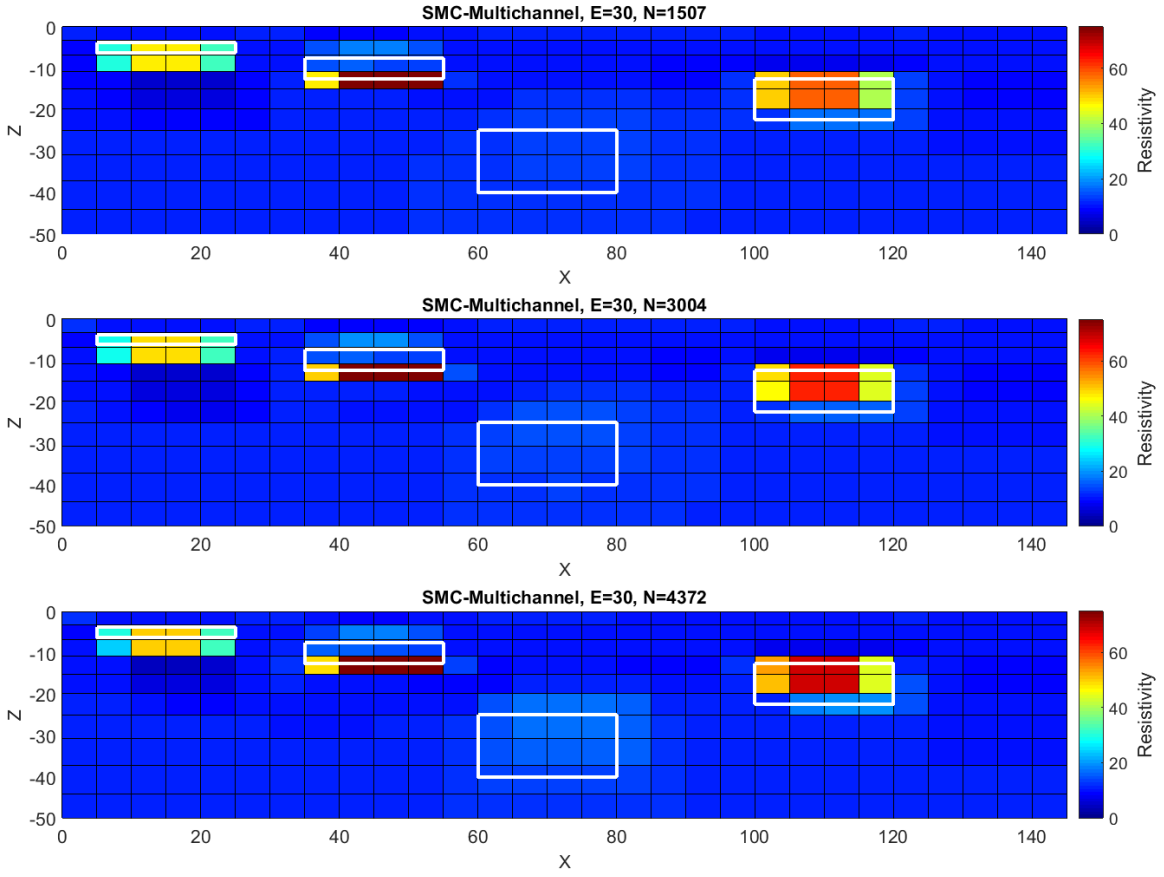

Figure 22: The modelblocks used for inverting simulated data and their inverted resisitivity value. The set of measurements is generated with the 'Spread Mass Center Multichannel' method. The total number of electrodes in the array is 30 spaced with 5 meters. Only every other electrode could be used for current injection and the rest could be used for potential readings leading to a total of 6585 possible measurements to choose from.

9.3 Effectiveness of Multichannel optimization

Below is a table of the different multichannel optimized methods average potential readings per current injection for the different cases discussed above.

	$N \approx 1500$	$N \approx 3000$	$N \approx 4368$
GradientXL, E=64	7.3978	-	-
MC, E=64	11.6154	11.2052	10.8193
SMCMC, E=64	11.2687	11.2351	11.2868
MC,E=30	10.0533	9.7000	9.3376
SMCMC, E=30	10.4653	10.1486	9.8914

Table 4: This table shows the average potential readings per current injection for the different scenarios and methods discussed, E is the number of electrodes in the layout and N is the number of measurements to take. Note that the 'GradientXL' protocol only has 1376 measurements while the other protocols have closer to 1500 measurements.

The multichannel system generally succeeds in allocating above 11 measurements per current injection for 64 electrodes. For 30 electrodes the number naturally shrinks due to fewer available measurements and the full switchboard is not in use (only the first two sections with electrodes 1-30 can be used, so there is only one a total of 4 switches.). The quality of the different kinds of measurements has not been explored specifically— measurements using a leaf electrode might be, in general, less informative than the measurements allocated in the main loop.

9.4 Field measurements

As the results presented above seem to indicate that the 'Spread mass center multichannel'-method is the best method of the ones discussed for taking multichannel optimized measurements it was tried in the field. The measurements were taken over an old quarry turned into a landfill. We expect big variation in the resistivity as the stone quarry is expected to have much higher resistivity compared to the trash. The true subsurface resistivity distribution is of course unknown so the results are compared with the 'GradientXL' standard protocol, also used to survey the same site. A total of 64 electrodes was used, space 5 meters apart. Some of the electrodes were excluded from the measurements either due to too bad electrode connection to the ground or due to the electrode position being covered in asphalt. The inverted data is shown below:

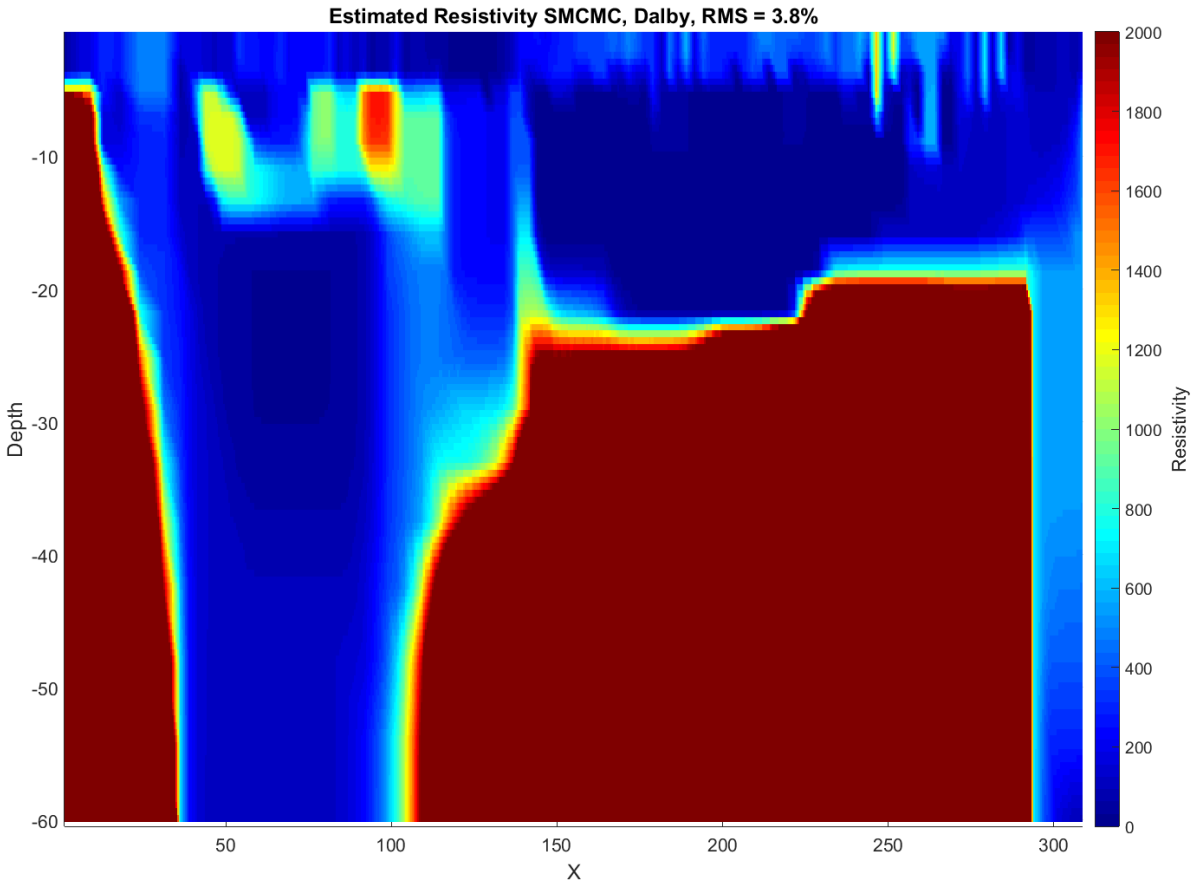

Figure 23: The inverted data from the Dalby measurement using the 'Spread mass centers multichannel'-method, the number of measurement was 1145. Note that this figure is heavily capped in order to compare to the 'GradientXL'-result. A uncapped figure is shown in 25

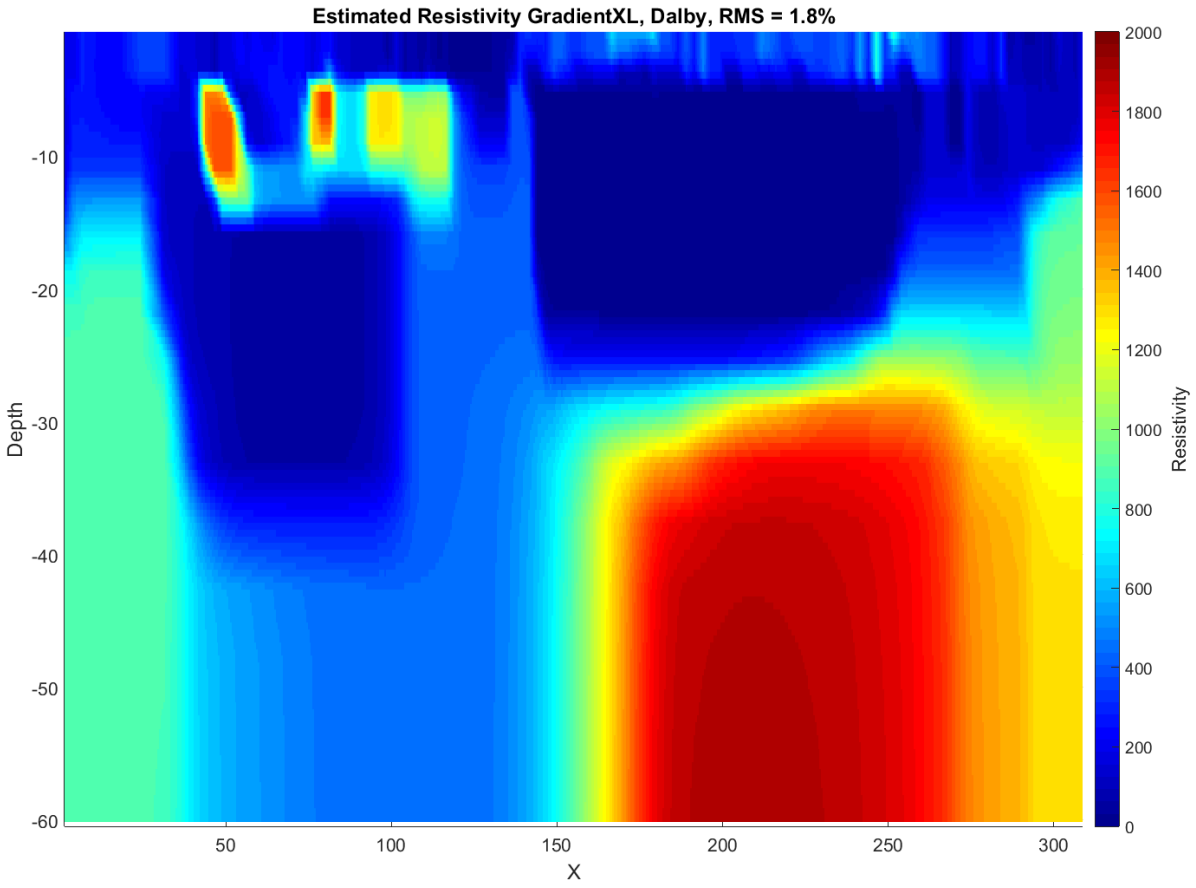

Figure 24: The inverted data from the Dalby measurement using the standard 'GradientXL'-protocol, the number of measurement was 1256.

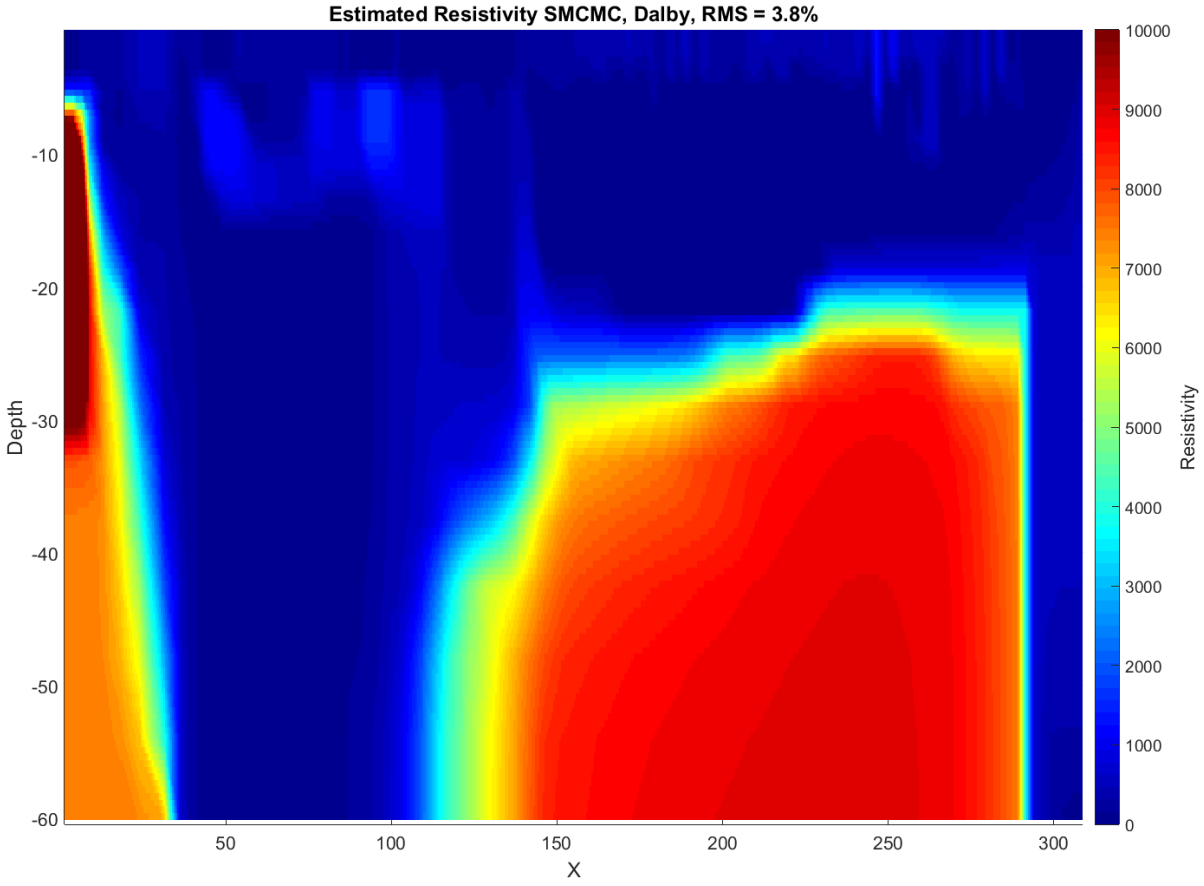

Figure 25: The inverted data from the Dalby measurement using the 'Spread mass centers multichannel'-method, the number of measurement was 1145.

The result seem to agree on some areas having high resistivity — they do not agree on the magnitude of the resistivity however. The 'Spread mass centers multichannel'-method has generally much higher resitivity values in the recognized prisms. I refrain from doing any geological interpretation of the result as I am no geologist. One thing that should be noted is that the SMCMC-survey was about 50% faster than the GradientXL-survey.

10 Conclusion

It seems clear that the results presented here would indiciate that the 'spread mass centers' method is the best approach for selecting measurement sequences of the methods discussed here. When comparing the results with the ones found [9] we should note that the parameters for the inversion process as well as the model of the ground might differ — it is more about a similar situation and how the different algorithms handle them. Qualitatively the spread of mass centers method, at least superficially with the consideration just discussed, perform about as well as the 'Compare R' method which is more computationally demanding.

Furthermore the multichannel scheduling successfully makes close to the maximum number of measurements per current injection leading to a survey time greatly reduced compared to using the standard 'gradientXL' protocol which is already partly optimized for multichannel use. The quality of the survey seems comparable, but further analysis by geological experts is needed.

We can also conclude that formulating simple optimization problems with easy solutions, such as the integral of the weighted sensitivity, perform underwhelmingly. This is most likely due to the fact that the methods does not incorporate any penalty to choosing multiple measurements in the same area nor measurements of the same type. This leads to the method choosing multiple high valued measurements that give information about the same area of the subsurface. For smaller problem were the selected number of measurements are close to the number of total measurements in the full set this might not be a big problem, but in these situations most methods of choosing a optimal measurement set will probably perform well. The only thing these methods have going for them is the speed with which they can be executed and they are of course useful to get a baseline of performance of optimized sets — if a method selecting an optimal measurements sequence does not outperform integral methods it is probably not worthwhile to continue developing the method.

The multichannel optimization algorithm succesfully allocates close to 12 electrode for every current injection for the 64 electrode layout. The usefulness of the leaf electrodes have however not been specifically examined in this article and it might be that an allocation of 8 electrodes per current injection might perform close to as good.

11 Outlook and further research

Although the results for the 'spread mass center' methods looks very promising for linear electrode layout and two dimensional models of the subsurface, the performance for more complex electrode layouts combined with 3D models of the subsurface has not been tested. For this kind of situation there are problems

with very different measurements having the same center of mass — this could potentially be rectified by modifying the method by for instance adding more dimensions in a clever way or by trying to find more than one 'mass center'. For the most part a measurement has two separate blocks of sensitivity from the different pole-pole pairs, so instead of using a single mass center it might be better to try and find the mass center of two different 'bodies'. The 'Spread mass centers'-method is also easily generalized to more general feature vectors describing each measurement. This should resolve the problem of seeing symmetric arrays in three dimensional problems as the same measurement when they are clearly not, but it might add computational complexity depending on how it is implemented. The method shows great promise as a relatively easy method for selecting well performing measurement sets.

The multichannel methods rely on solving the optimization problem presented in (65) for suitable scores. In this article only electrode layouts of at most 64 electrodes have been studied and the problem in (65) and the simplified switchboard has been specifically designed to handle this kind of layouts. For larger layouts with more electrodes modification is necessary but the general idea might still be worthwhile exploring.

In order to evaluate the result many different methods of selecting measurement sets needs to be implemented and the result of simulations needs to be compared. This is useful because it will also give an indication of the real world performance. Alternative evaluations give a quantitative score for each measurement set [8], but the resulting simulations are less useful for gauging real world performance as the inversion models can perfectly match the synthetic model (meaning that there are no artifacts from misalignment between parameters of the inversion model and synthetic model — they represent the exact same thing). One interesting future research project might be to use quantitative performance measurements and evaluate measurement sets both compared to each other but more importantly with a random measurement set selecting each measurement with equal probability. Basically a Monte-Carlo simulation for the expected performance of a random measurement set could be studied to determine if *any* of the measurement strategies presented here or in previously conducted research can be clearly distinguished from a random measurement set. If they can not be distinguished from a random measurement set the only important thing is optimizing for multichannel usage without introducing bias.

References

[1] A. Binley. 11.08 - tools and techniques: Electrical methods. In Gerald Schubert, editor, *Treatise on Geophysics (Second Edition)*, pages 233 – 259. Elsevier, Oxford, second edition edition, 2015.

[2] Frederick J. Milford John R. Reitz and Robert W. Christy. Chapter 7-

electric current. In *Foundations of Electromagnetic Theory (Third Edition)*, pages 135 – 160. Addison-Wesley, third edition edition, 1979.

[3] M. H. Loke and R. D. Barker. Least-squares deconvolution of apparent resistivity pseudosections. *GEOPHYSICS*, 60(6):1682–1690, 1995.

[4] M.H. Loke, P.B. Wilkinson, J.E. Chambers, S.S. Uhlemann, and J.P.R. Sorensen. Optimized arrays for 2-d resistivity survey lines with a large number of electrodes. *Journal of Applied Geophysics*, 112:136 – 146, 2015.

[5] P. R. McGillivray and D. W. Oldenburg. Methods for calculating frechet derivatives and sensitivities for the non-linear inverse problem: a comparative study. *Geophysical Prospecting*, 38(5):499–524, 1990.

[6] Dr. M.H.Loke. *Tutorial : 2-D and 3-D electrical imaging surveys*. 1996-2016.

[7] Stephen K. Park and Gregory P. Van. Inversion of pole-pole data for 3-d resistivity structure beneath arrays of electrodes. *Geophysics*, 56(7):951–960, 1991.

[8] Paul B. Wilkinson, Meng Heng Loke, Philip I. Meldrum, Jonathan E. Chambers, Oliver Kuras, David A. Gunn, and Richard D. Ogilvy. Practical aspects of applied optimized survey design for electrical resistivity tomography. *Geophysical Journal International*, 189(1):428–440, 2012.

[9] Paul B. Wilkinson, Philip I. Meldrum, Jonathan E. Chambers, Oliver Kuras, and Richard D. Ogilvy. Improved strategies for the automatic selection of optimized sets of electrical resistivity tomography measurement configurations. *Geophysical Journal International*, 167(3):1119–1126, 2006.